T.C.
BAHÇEŞEHİR UNIVERSITY

GENOTYPE-PHENOTYPE CORRELATION OF IDH MUTATIONS IN GLIAL TUMORS

Master's Thesis

GİZEM TURAN

İSTANBUL, 2019

T.C.

BAHÇEŞEHİR UNIVERSITY

GRADUATE SCHOOL OF HEALTH SCIENCES

NEUROSCIENCE

GENOTYPE-PHENOTYPE CORRELATION OF IDH MUTATIONS IN GLIAL TUMORS

Master's Thesis

GİZEM TURAN

Supervisor: Assist. Prof. Dr. Timuçin Avşar

İSTANBUL, 2019

THE REPUBLIC OF TURKEY
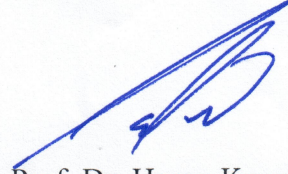**BAHCESEHIR UNIVERSITY**

GRADUATE SCHOOL OF HEALTH SCIENCES
NEUROSCIENCE

Name of the thesis: Genotype-phenotype correlation of IDH mutations in glial tumors
Name/Last Name of the Student: Gizem Turan
Date of the Defense of Thesis: 21.03.2019

The thesis has been approved by the Graduate School of Health Sciences.

Assoc. Prof. Dr. Hasan Kerem ALPTEKİN
Graduate School Director
Signature

This is to certify that we have read this thesis and we find it fully adequate in scope, quality and content, as a thesis for the degree of Master of Science.
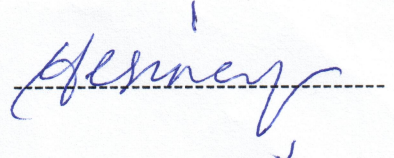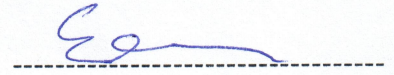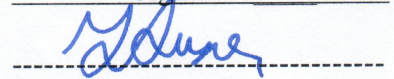
Examining Comittee Members   Signature

Thesis Supervisor
Assist. Prof. Dr. Timuçin AVŞAR

Member
Prof. Dr. Eda TAHİR TURANLI

Member
Assoc. Prof. Dr. Yeşim NEĞİŞ

ABSTRACT

GENOTYPE-PHENOTYPE CORRELATION OF IDH MUTATIONS IN GLIAL TUMORS

Gizem TURAN

Neuroscience Master Program

Thesis Supervisor: Assist. Prof. Dr. Timuçin AVŞAR

March 2019, 48 pages

Glioma brain tumors are the most common of the central nervous system tumors. Treatments of these tumors can be performed using treatments methods such as surgical resection, chemotherapy, and radiation, but no successful results can be always obtained after treatment. Therefore, the classification of these tumors is significant for the accurate and effective administration of the treatment. IDH1 and IDH2 mutations have been used as important molecular markers due to their good prognosis effects on gliomas with the 2016 World Health Organization (WHO) classification.

The mutated IDH1/2 enzymes gain a neomorphic function, resulting in the overproduction of 2HG oncometabolite, which induces significant changes in the cell by partially inhibiting very essential cell mechanisms. These changes, especially epigenetic alterations, affect cell proliferation, differentiation, and metabolism.

The fact that the good prognosis effect of the IDH1 mutations in glial tumors is still not fully explained and the results found in previous studies on this subject are conflicting, have encouraged us to do this study. In this study, for the observation of these effects, studies on cell proliferation and migration were performed by using R132H, R132C, R132S, and R132L amino acid changes in IDH1 enzyme. As a result of our studies, except for G395A mutation which caused R132H amino acid change, it was seen that while other mutations decreased cell proliferation, only C394T mutation continued to show this effect in repeated studies with different cell line. On the other hand, no effect of these mutations on cell migration was observed.

Keywords: Gliomas, IDH1 Mutations, Prognosis

ÖZET

GENOTYPE-PHENOTYPE CORRELATION OF IDH MUTATIONS IN GLIAL TUMORS

Gizem TURAN

Sinirbilimi Yüksek Lisans Programı

Tez Danışmanı: Dr. Öğr. Üyesi Timuçin AVŞAR

Mart 2019, 48 sayfa

Glioma beyin tümörleri, merkezi sinir sistemi tümörlerinin en yaygın olanıdır. Bu tümörlerin tedavileri, cerrahi rezeksiyon, kemoterapi ve radyasyon gibi tedavi yöntemlerinin uygulanmasıyla yapılabilmektedir, fakat tedavi sonrası her zaman başarılı bir sonuç alınamamaktadır. Bu nedenle, bu tümörlerin sınıflandırılması tedavinin doğru ve etkili bir şekilde uygulanması açısından önem taşımaktadır. 2016 Dünya Sağlık Örgütü (WHO) sınıflaması ile IDH1 ve IDH2 mutasyonları, gliomalarda iyi prognoz etkilerinden dolayı önemli moleküler belirteçler olarak kullanılmaya başlanmıştır.

Mutasyon içeren IDH1/2 enzimleri, yeni fonksiyon kazanarak aşırı miktarda 2HG onko metabolitin üretilmesine sebep olmaktadırlar ve bu metabolit çok önemli hücre mekanizmalarını kısmen inhibe ederek hücre içerisinde önemli değişiklikleri meydana getirmektedir. Bu değişiklikler, özellikle epigenetik ile ilgili olan değişiklikler, hücrenin proliferasyonunu, farklılaşmasını ve metabolizmasını etkilemektedir.

IDH1 mutasyonlarının glial tümörlerindeki iyi prognoz etkisinin hala tam olarak açıklanamamış olması ve bu konuda yapılan önceki çalışmalarda bulunan sonuçların çelişkili olması bu çalışmayı yapmamız açısından teşvik edici olmuştur. Bu çalışmada, bu etkileri gözlemleyebilmek için IDH1 enzimindeki R132H, R132C, R132S ve R132L amino asit değişimleri kullanılarak hücre proliferasyonu ve migrasyonu üzerine çalışmalar yapılmıştır. Çalışmalarımız sonucunda, R132H amino asit değişimine sebep olan G395A mutasyonu haricinde diğer mutasyonların proliferasyonu azalttığı görülmesine rağmen, farklı hücre hattıyla tekrarlanan çalışmalarda sadece C394T mutasyonu bu etkisini göstermeye devam etmiştir. Diğer yandan bu mutasyonların hücre migrasyonu üzerine etkisi gözlemlenmemiştir.

Anahtar Kelimeler: Gliomalar, IDH1 Mutasyonları, Prognoz

TABLE OF CONTENTS

TABLES

FIGURES

ABBREVIATIONS

αKG	:	Alpha-Ketoglutarate
2HG	:	2-Hydoxyglutarate
2OG	:	2-Oxoglutarate
AITL	:	Angioimmunoblastic T-cell lymphoma
AML	:	Acute myelogenous leukemia
CAC	:	Citric Acid Cycle
CBTRUS	:	Central Brain Tumor Registry of the United States
CNS	:	Central Nervous System
CT	:	Computed Tomography
DNA	:	Deoxyribonucleic acid
dNTP	:	Deoxynucleotide Triphosphate
EGFP	:	Enhanced Green Fluorescent Protein
G-CIMP	:	Glioma CpG Island Methylator Phenotype
GBM	:	Glioblastoma
HGG	:	High-Grade Glioma
IDH	:	Isocitrate Dehydrogenease
LGG	:	Low-Grade-Glioma
MGMT	:	O6-methylguanine-DNA-methyltransferase
MRI	:	Magnetic Resonance Imagining
NADPH	:	Nicotinamide adenine dinucleotide phosphate
NOS	:	Not otherwise specified
PEI	:	Polyethyleminine
ROS	:	Reactive oxygen species
TCA	:	Tricarboxylic Acid
TERT	:	Telomerase reverse transcriptase
TET	:	Ten-eleven translocation
WHO	:	World Health Organization

SYMBOLS

Alpha   : α

Carbon dioxide   : C_2O

Sodium chloride   : NaCl

1. INTRODUCTION

Central nervous system (CNS) tumors account for approximately 3 percent of all cancer types (Yeole, 2008), however despite this low rate these tumors have very significantly high morbidity and mortality rate. In addition, CNS tumors cause severe symptoms as headache, nausea, seizures and mental alterations. These symptoms are generally considered as signs of these tumors in the initial examination (Buckner et al., 2007).

Gliomas, which are present about 80.7 percent in malignant primary brain tumors, are the most common type of central nervous system (CNS) tumors (Ostrom et al., 2017). Although these tumors exhibit different degrees of malignant properties, the common features are that treatments of gliomas are usually difficult. After treatment such as surgical resection, chemotherapy, and radiation, the recurrent of these tumors is considerably common, and as a result of this, the survival rate in gliomas is affected adversely. Furthermore, GBM, which is grade IV according to the grading system of WHO classification, is the most aggressive form of gliomas and the survival rate in these tumors is very low (Deng et al., 2018).

Unlike the 2007 WHO glioma classification, in the 2016 WHO classification of gliomas molecular parameters such as IDH mutations, 1p/19q codeletion, MGMT promoter methylation, TERT promoter mutations, and EFGR alterations were based on, and these molecular parameters have been identified as crucial molecular markers in gliomas, especially due to their effects on prognosis (Louis et al., 2016).

The mutations in isocitrate dehydrogenases (IDH) genes are present in approximately 12 percent GBMs and 80-90 percent grade II and III astrocytomas, oligodendrogliomas, and oligoastrocytoma (Aquilanti et al., 2018). The critical role of IDHs mutations in gliomas in terms of the clinical evaluation of the tumor is that these tumors exhibit favorable prognosis compared to gliomas with IDH wildtype, therefore these mutations are used routinely as a significant molecular marker of gliomas (Louis et al., 2016).

Mutated IDH1/2 enzymes gain a new enzymatic function which is the production of 2HG from αKG instead of the conversion of αKG to isocitrate (Dang et al., 2009). The accumulation of 2HG that is proven to be an oncometabolite affects the essential mechanisms as cellular metabolism, redox states, DNA repair, and epigenetic changes (Al-Khallaf, 2017).

Due to 2HG-dependent epigenetic alterations, the IDH1/2 mutations can affect cell differentiation, proliferation, metabolism, and survival. The reason is that IDH1/2 mutations disrupt the histone methylation patterns that influence the expression of tumor suppressor genes, oncogenes, and metabolic genes through the changes in DNA methylation and post-translational histone modifications (Turcan et al., 2012).

Since the identification of the effects of IDH1/2 mutations on good prognosis in gliomas, there has been increased research on how these mutations contribute to tumor formation by altering cell metabolism. In previous studies, it was investigated that the effects of IDH mutations and the overaccumulation of the 2HG metabolite in cell metabolism on proliferation, migration, and tumor formation (Lu et al., 2012).

In our study, it was aimed that evaluate the effects of IDH1 mutations (R132H, R132C, R132S, R312L) on phenotype behaviors as migration and proliferation. In previous studies on gliomas, the phenotype effects of R132H, that is the most prevalent amino acid change in IDH1 mutations, have been investigated. In these studies, there were no clear conclusions about how this mutation exactly affects proliferation and migration, and this has been interpreted that the results can change based on different tumor types and different cell lines. In our study, studies were conducted on cell lines because the less common mutations in glioma tumors would be looked for and, therefore, the tumor sample containing these mutations could be difficult to find. The amino acid alterations as R132H, R132C, R132S, R312L were performed into IDH1 wild-type plasmid by Site-Directed Mutagenesis method, and the study continued with the transfer of these plasmids into the cells. Following this, migration and proliferation assays were performed to observe the phenotype effects.

2. LITERATURE REVIEW

2.1 CENTRAL NERVOUS SYSTEM TUMORS

Central nervous system tumors are formed by the division of abnormal cells without control in the brain and spinal cord tissues. Headache, seizures, and mental changes are the most prevalent signs and symptoms of these tumors. Radiological examinations such as magnetic resonance imagining (MRI) and computed tomography (CT) are usually used for the diagnosis of CNS tumors (Buckner et al., 2007).

These brain tumors are divided into two main groups as benign tumors that are noncancerous and rarely invade other tissues, and malignant tumors that are cancerous and aggressively spread into other tissues. In addition, CNS tumors are classified into two groups according to their formation as primary and secondary tumors.

Primary brain tumors that can be benign or malignant occur directly in the brain and rarely spread to other organs of the body. Although benign primary brain tumors generally grow slowly and do not tend to spread, they can cause possible symptoms by pressure on the parts of the brain. Also, these benign tumors may change over time and turn into malignant tumors (Behin et al., 2003). The origin of primary malignant brain tumors is brain tissues, but the difference between these tumors and benign tumors is that they can invade easily to healthy brain tissues. In malignant primary brain tumors that is one of the most difficult neoplasms to treat, the overall 5-year survival is not more than 35 percent. Besides, it is known that the most occurred malignant primary brain tumor in adults is gliomas (Lapointe et al., 2018).

Secondary brain tumors (metastatic brain tumors) formed by the metastasis of other tissues in the body to the brain are malignant. Secondary brain tumors, which are more common than primary brain tumors, are frequently caused by the spread of lung cancer, breast cancer, skin cancer, kidney cancer, and colon cancer (DeAngelis, 2001).

Central nervous system tumors constitute less than ~ 3 percent of all cancers (Yeole, 2008). Although this percentage seems to represent a small number, this tumor has a significant proportion in terms of morbidity and mortality (Buckner et al., 2007). In addition, the most prevalent CNS tumors are meningiomas in the benign brain tumors and glioblastoma in the malignant brain tumors, and also these two brain tumors are most commonly diagnosed at older ages (Ostrom et al., 2017).

2.2 GLIOMAS

Gliomas, which represent the most common primary intracranial brain tumors in adults, are neoplasms originating from the glial cells or supporting cells. Glioma being heterogeneous cancer with various subtypes comprises ependymoma, astrocytoma, oligodendroglioma, and oligoastrocytoma (mixed glioma) according to histological features (Lapointe et al., 2018).

In the World Health Organization (WHO) classification, malignant gliomas are categorized as low-grade gliomas (LGGs; grade II) and high-grade gliomas (HGGs; grade III, IV), based on their histological properties. The differentiation between these two groups is of great importance in terms of prognosis and treatment approaches, such as administration of adjuvant radiation and chemotherapy following surgical resection in high-grade gliomas. On the other hand, a patient with low-grade glioma may be misdiagnosed as a high-grade glioma and applied seriously aggressive treatment (Togao et al., 2015).

Gliomas account for ~ 80.7 percent of malignant primary brain tumors and ~ 26.5 percent of all primary brain tumors. Glioblastoma (GBM) with a very low survival rate comprises 56.1 percent of gliomas (Figure 2.1). According to the report published by Central Brain Tumor Registry of the United States (CBTRUS), the incidence of glioblastoma, the highest incidence rate for malignant CNS tumors, has been reported as 3.20 per 100,000 population between 2010 and 2014, followed by diffuse astrocytoma with the incidence rate of 0.48 per 100,000 population (Ostrom et al., 2017).

Figure 2.1: The distribution of gliomas by histology subtypes
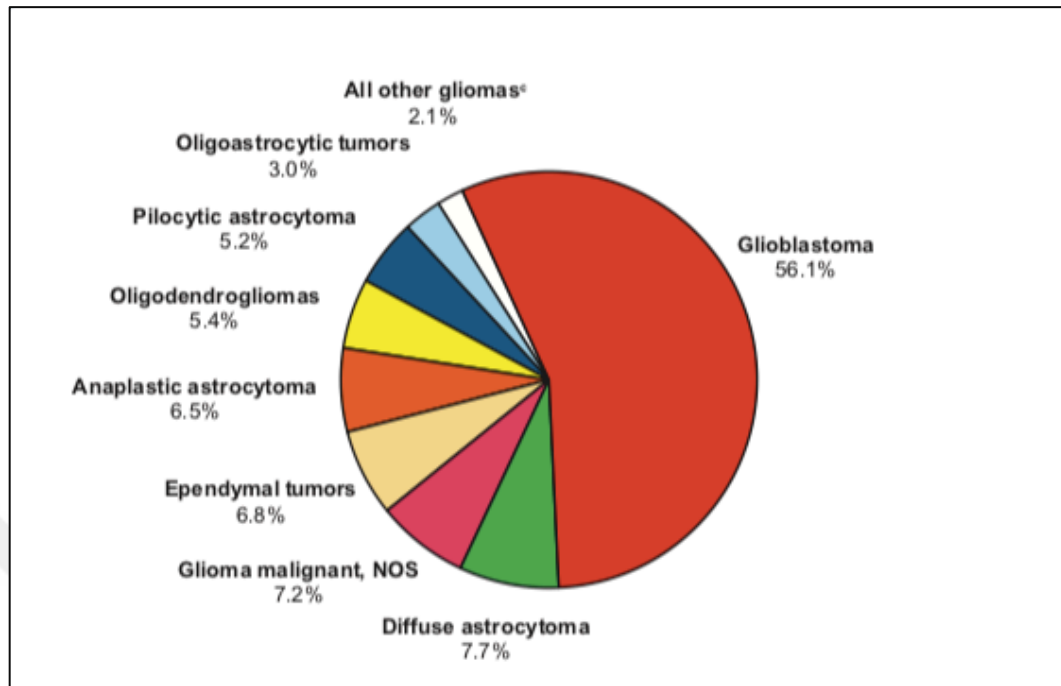
Reference: Ostrom, Q. T., Gittleman, H., Liao, P., Vecchione-Koval, T., Wolinsky, Y., Kruchko, C. & Barnholtz-Sloan, J. S. 2017. CBTRUS statistical report: primary brain and other central nervous system tumors diagnosed in the United States in 2010–2014. *Neuro-oncology,* 19, v1-v88.

2.2.1 Glioma Classification

The classification of gliomas which is a prevalent tumor type among malignant brain tumors and have a high morbidity and mortality rate is important for accurate determination and effective application of treatment.

Until 2016, the WHO classification of brain neoplasms has been made generally according to histological characteristics by using microscopic features. In this classification, glial tumors were classified from benign to malignant by evaluating histological features such as cellular atypia, cell density, endothelial proliferation, mitosis, and necrosis. The histological grading system has a critical role in the clinical setting, especially in determining the methods of administration of therapies as adjuvant radiation and specific chemotherapy treatments (Louis et al., 2007).

Grade I gliomas are usually benign tumors with low proliferative potential and can only be treated by surgical resection. Grade II gliomas, called diffuse infiltrative gliomas, have low proliferative activity, they can frequently recur and even turn into high-grade malignancy. Grade III gliomas are invasive and also more aggressive than grade I and grade II. Grade IV glioma, also known as glioblastoma (GBM), which represents the most common malignant primary brain tumors in adults, is the most aggressive grade form and related with poor prognosis (DeAngelis, 2001, Deng et al., 2018).

According to the 2016 report of WHO classification of CNS tumors, the classification of gliomas has reformed by having regard to molecular parameters, and this revised classification has significant effects on the enhancement of diagnostic approaches, prognosis, and treatment planning (Wesseling and Capper, 2018).

One of the most prominent of this classification from 2007 WHO classification is that all astrocytic tumors have been categorized in the same group in the 2007 classification, whereas all diffuse infiltrative gliomas are grouped together in this new classification. In order to classify the diffuse gliomas in this manner, both histologically the growth morphology and behavior of the tumor and the shared genetic driver mutations in the IDH1 and IDH2 genes were based (Figure 2.2). Diffuse astrocytoma (grade II) and anaplastic astrocytoma (grade III) are classified into IDH-mutant, IDH-wildtype and NOS (the not otherwise specified) groups in the 2016 classification. The diagnosis of diffuse astrocytoma, IDH-wildtype and anaplastic astrocytoma, IDH-wildtype is observed rarely (Louis et al., 2016). Glioblastomas are divided into three groups: glioblastoma, IDH-wildtype, glioblastoma, IDH-mutant and glioblastoma, NOS. Glioblastoma, IDH-wildtype has seen mostly in patients over 55 years of age is named primary glioblastoma or de novo glioblastoma. Also, Glioblastoma, IDH-mutant defined as secondary glioblastoma is associated with a history of formerly low-grade diffuse gliomas and appears in preferably younger patients (Ohgaki and Kleihues, 2013). Glioblastoma, NOS is a category used for tumors which full assessment of IDH cannot be implemented. Glioblastoma, IDH-wildtype is more frequently found than Glioblastoma, IDH-mutant. Grade II oligodendroglioma and grade III anaplastic

oligodendroglioma are now categorized by considering the combination of IDH mutation and 1p/19q codeletion used in the diagnosis of these tumors (Louis et al., 2016).

Figure 2.2: Histological and molecular classification of diffuse gliomas
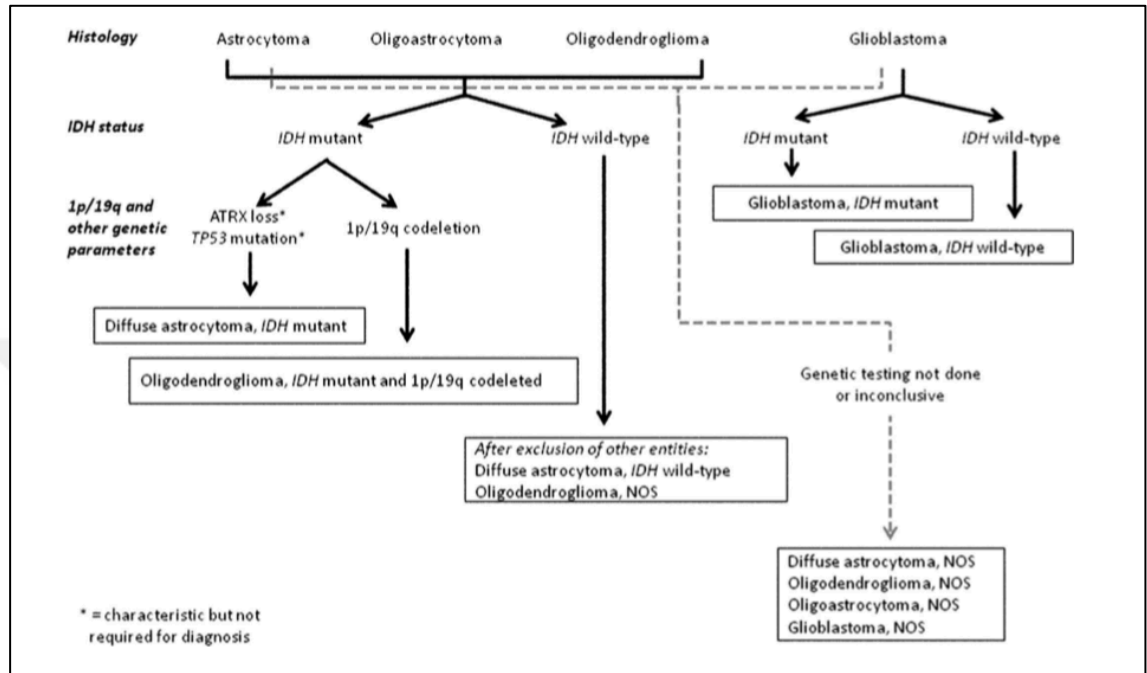
Reference: Louis, D. N., Perry, A., Reifenberger, G., Von Deimling, A., Figarella-Branger, D., Cavenee, W. K., Ohgaki, H., Wiestler, O. D., Kleihues, P. & Ellison, D. W. 2016. The 2016 World Health Organization classification of tumors of the central nervous system: a summary. *Acta neuropathologica,* 131, 803-820.

In the 2016 classification, molecular information was added to the histopathological names by changing the terminology with the addition of molecular parameters (Louis et al., 2016). According to this last published report, the histopathological names of gliomas, their grades, and their molecular information are shown in Table 2.1.

Table 2.1: Tumor grades of selected gliomas according to the 2016 WHO classification

	Grades
Diffuse astrocytic and oligodendroglial tumors	
Diffuse astrocytoma, IDH-mutant	II
Anaplastic astrocytoma, IDH-mutant	III
Glioblastoma, IDH-wildtype	IV
Glioblastoma, IDH-mutant	IV

	Grades
Diffuse astrocytic and oligodendroglial tumors	
Diffuse midline glioma, H3K27M-mutant	IV
Oligodendroglioma, IDH-mutant and 1p/19q-codeleted	II
Anaplastic oligodendroglioma, IDH-mutant and 1p/19q-codeleted	III
Other astrocytic tumors	
Pilocytic astrocytoma	I
Subependymal gliant cell astrocytoma	I
Pleomorphic xanthoastrocytoma	II
Anaplastic pleomorphic xanthoastrocytoma	III
Eppendymal tumors	
Subependymoma	I
Myxopapillary ependymoma	I
Ependymoma	II
Ependymoma, *RELA* fusion-positive	II or III
Anaplastic ependymoma	III
Other gliomas	
Angiocentric glioma	I
Chordoid glioma of third ventricle	II

Reference: This table was prepared by Gizem TURAN based on literature (Louis, D. N., Perry, A., Reifenberger, G., Von Deimling, A., Figarella-Branger, D., Cavenee, W. K., Ohgaki, H., Wiestler, O. D., Kleihues, P. & Ellison, D. W. 2016. The 2016 World Health Organization classification of tumors of the central nervous system: a summary. *Acta neuropathologica,* 131, 803-820.)

2.2.2 Molecular Markers of Gliomas

2.2.2.1 IDH mutations

The mutations in isocitrate dehydrogenases (IDH) genes cause overaccumulation of oncometabolite 2-hydroxyglutarate (2-HG) which affects cellular mechanisms in tumor cells, especially the epigenetic state (Dang et al., 2009). It was proved in previous studies in the literature that IDH1 mutations can be determined in approximately 80-90 percent of

astrocytic and oligodendroglial (grade II and grade III) gliomas and in 12 percent GBMs (Aquilanti et al., 2018). The different variants of IDH1 mutations can also occur in gliomas as R132C, R132S, R132G, and R132L, despite detection of IDH1 R132H mutation version mostly (Hartmann et al., 2009). Also, IDH2 mutations that are rarely observed than IDH1 mutations (Yan et al., 2009) in gliomas are commonly found in oligodendrogliomas. DNA sequencing and immunohistochemistry (IHC) are applied routinely as detection methods for IDH mutations. The effect of IDH mutations on prognosis in gliomas is more significant compared to other molecular markers, and the presence of mutant IDH is related to favorable prognosis in gliomas (Aquilanti et al., 2018).

2.2.2.2 1p/19q codeletion

Chromosome 1p/19q codeletion, which is the result of an unbalanced translocation between the entire arms, has been associated with oligodendrogliomas (Aquilanti et al., 2018). Although it has been identified for a long time that 1p/19q codeletion has a good effect on the prognosis of gliomas, its role in the molecular mechanism of the tumor has not been completely identified (AVŞAR and KILIÇ). This 1p/19q codeletion co-occurs with IDH mutation, and this combination of molecular alterations provide the longest survival compared with IDH mutant alone and IDH wildtype. FISH, SNP microarrays, or NGS techniques can be applied to investigate the presence of the 1p/19q codeletion for a diagnosis of oligodendroglioma (Wesseling and Capper, 2018).

2.2.2.3 MGMT promoter methylation

O6-methylguanine-DNA-methyltransferase (MGMT) which eliminates alkyl groups from the O6 part of guanine is a DNA repair enzyme (Esteller et al., 2000). Alkylating chemotherapeutics can alter the O6 position of guanine during chemotherapy treatment, and therefore this repair mechanism provides that MGMT removes the adverse effect of temozolomide (TMZ) used in chemotherapy for GBM and grade II and grade III gliomas. The hypermethylation of MGMT promoter cause the silence of MGMT expression, and so the effect of TMZ on the treatment of gliomas increases by removing of the resistance

effect of MGMT on TMZ (Hegi et al., 2004). In short, MGMT promoter hypermethylation provides good prognosis in gliomas. This prognostic marker for gliomas is routinely detected with IHC method (Aquilanti et al., 2018).

2.2.2.4 TERT promoter mutations

While telomerase is an enzyme that enables the maintenance and the prolongation of telomeres at chromosome ends, telomerase reverse transcriptase (TERT) is the catalytic subunit of telomerase. Normally, telomeres shorten with each cell division and provide a defined lifespan length of any cell, whereas TERT promoter mutations exhibit telomerase reactivation in cancer cells and these cells gain limitless proliferative capabilities (Huang et al., 2013). TERT promoter mutations are generally supportive for diagnosis of IDH wildtype diffuse astrocytoma, anaplastic astrocytoma, glioblastoma or IDH-mutant and 1p/19q codeleted oligodendroglioma (Eckel-Passow et al., 2015). The detection of TERT promoter mutations associated with poor prognosis is not performed routinely, but these mutations can be determined by using DNA sequencing techniques (Aquilanti et al., 2018).

2.2.2.5 EGFR alterations

Epidermal growth factor receptor (EGFR) is associated with cell division, apoptosis control, and cell invasion. The overexpression of EGFR induced mutations lead to a poor prognosis in gliomas, particularly GBM (Aquilanti et al., 2018), and EGFR alterations are found in about 40-50 percent GBM, IDH wildtype (Wen and Kesari, 2008). Although there is no continuous detection method used to define the EGFR alterations, DNA sequencing panels can be utilized to detect these mutations (Aquilanti et al., 2018).

2.3 THE MUTATIONS OF IDH1/IDH2 IN GLIOMAS

IDHs (Isocitrate dehydrogenases) are metabolic enzymes that play a crucial role in cellular metabolism, epigenetic regulation, redox states, and DNA repair (Al-Khallaf, 2017). In human, there are three isoforms of IDH enzymes: IDH1, IDH2, and IDH3 (Reitman and Yan, 2010). IDH1 is found in the cytosol and peroxisome, whereas IDH2

and IDH3 are located in the mitochondrial matrix. The mutations of IDH1 and IDH2 in tumors are different from the other isoform IDH3, which is an NAD^+-dependent enzyme since the mutations of IDH3 in tumors are not driver mutations. As the reason for this, mutations in the IDH3 enzyme are inactivated in such a way that they have no potential to form cancer due to the structure of IDH3 and the irreversible reaction catalyzed by IDH3 (Al-Khallaf, 2017).

Mutations in $NADP^+$-dependent IDH1 (chromosome 2q34) and IDH2 (chromosome 15q26.1) enzymes are present in different tumor types at distinct frequencies such as malignant gliomas (~ 80-90 percent), acute myelogenous leukemia (AML) (~ 10-30 percent), angioimmunoblastic T-cell lymphoma (AITL) (~10-40 percent), chondrosarcoma (~ 50-70 percent), and cholangiocarcinoma (~ 10-20 percent) (Losman and Kaelin, 2013). In glioma tumors, these mutations are frequently related to grade II-III gliomas and secondary glioblastomas (Choi et al., 2016). Furthermore, as the frequency of these mutations, IDH1 mutations are more common in these glioma tumors types than IDH2 mutations, and in contrast, IDH2 mutations occur prevalently in AML in comparison with IDH1 mutations.

2.3.1 Normal Function of IDH1/IDH2

IDH1 and IDH2 enzymes that are homodimeric $NADP^+$-dependent enzymes catalyze the reversible oxidative decarboxylation of isocitrate to αKG in the tricarboxylic acid (TCA) cycle, also known as the Krebs cycle or the citric acid cycle (CAC) (Figure 2.3). During this process, $NADP^+$ is reduced to NADPH and CO_2 is produced (Reitman and Yan, 2010). In this reversible reaction, the orientation of reaction is highly associated with the relative levels of the isocitrate and αKG (also known as 2-oxoglutarate [2-OG]) and the relative Km values of the forward and reverse reactions (Lemons et al., 2010).

IDH1 has a role to provide the activity of cytoplasmic and nuclear dioxygenases that use the αKG as a co-substrate (Hausinger, 2004). The reaction of the production αKG in TCA cycle is a reversible reaction, so IDH1 is able to catalyze the isocitrate production and then, this can support the lipid biosynthesis (Filipp et al., 2012). IDH1 is an important

source of nonmitochondrial NADPH which is a crucial antioxidant that provides the protection of cells by preventing the oxidative stress and radiation damage (Kim et al., 2007). On the other hand, IDH2 contributes to the energy metabolism by regulating the amounts of isocitrate and αKG in the mitochondria (DeBerardinis et al., 2008). Also, IDH2 has a protective function against mitochondrial-oxidative stress by producing NADPH (Lee et al., 2007).

Figure 2.3: The IDH family enzymes in Krebs cycle
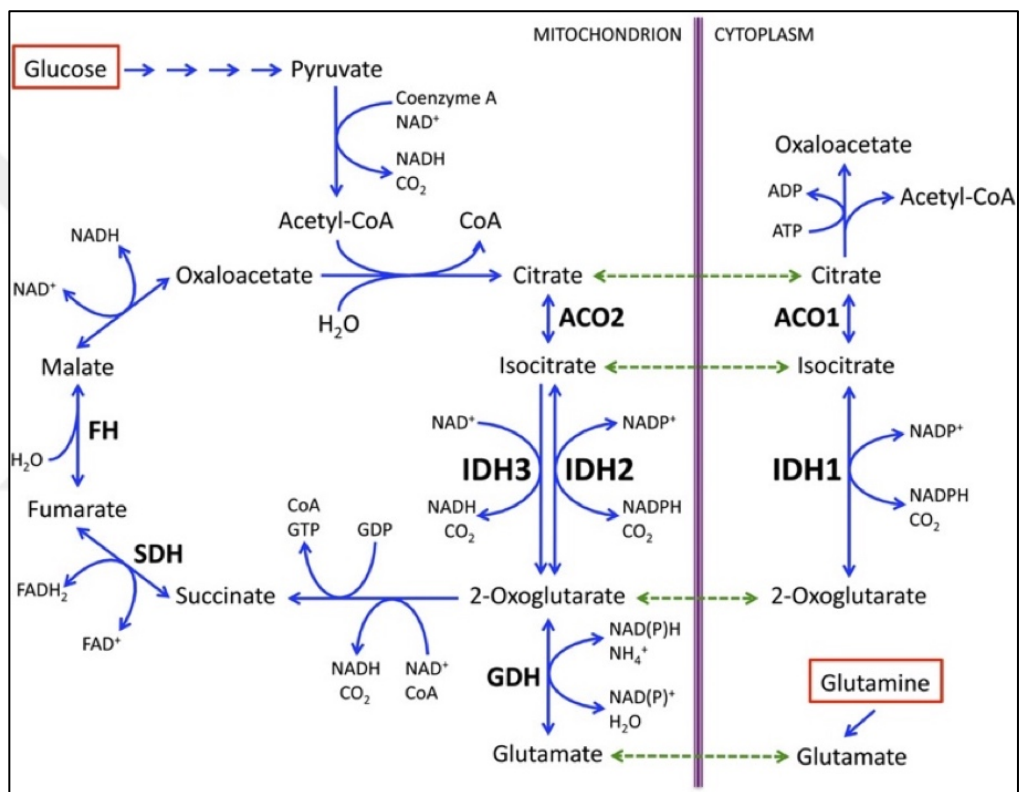
Reference: Losman, J.-A. & Kaelin, W. G. 2013. What a difference a hydroxyl makes: mutant IDH,(R)-2-hydroxyglutarate, and cancer. *Genes & development,* **27,** 836-852.

2.3.2 IDH1/IDH2 Mutations in Gliomas

Somatic mutations in IDH1 and IDH2 genes have been found in astrocytomas, oligodendrogliomas, oligoastrocytoma, and secondary GBM. These mutations, which have become important as molecular markers with 2016 WHO classification, have been shown to have a good prognosis effect on glioma tumors (Louis et al., 2016).

When IDH mutations were first defined in tumor cells, it was supposed that these mutations caused a loss of function and the inhibition of wild-type IDH activity. Therefore it was concluded that these mutations contribute to tumorigenesis because of this loss of function (Yan et al., 2009, Zhao et al., 2009). However, cancer-associated IDH1 and IDH2 mutations have proven to cause a neomorphic enzymatic gain of function (Dang et al., 2009). The mutations are located in R100 and R132 sites of IDH1, and R140 and R172 sites of IDH2. These residues, which are the active sites of the enzymes, compose hydrogen bonds to mediate binding of isocitrate (Xu et al., 2004). Mutations in these sites lead to reduce the binding affinity of the enzyme for isocitrate and promote the binding affinity of the enzyme for NADPH, that dramatically removes the oxidative decarboxylation activity of the enzymes (Dang et al., 2009). In addition to these effects of mutations, the conformation of the enzyme active site is altered because of mutations at these residues. Due to this conformational change, the conversion of 2-OG to isocitrate is prevented, and 2-OG produces (R)-2HG instead of isocitrate. In brief, IDH mutations result in high production and accumulation of 2HG, which support that IDH mutations cause the enzyme to gain a new function, not a loss of function (Losman and Kaelin, 2013).

The most prevalent amino acid change in IDH1 is R132H with about 70.9 percent in WHO grades II and III gliomas whereas, IDH2 mutations in these tumor types are found approximately 3.1 percent. Other amino acid changes in IDH1 than R132H are R132C, R132S, R132G, and R132L, respectively. In the 2009 study of Hartmann et al., the distribution of both these amino acid changes found in IDH1 and the amino acid alterations observed in IDH2 were showed after the screening of 1,010 astrocytomas, oligodendrogliomas, and oligoastrocytomas (Figure 2.4) (Hartmann et al., 2009).

Figure 2.4: The distribution of IDH1 and IDH2 mutations in 1,010 WHO grade II and III astrocytomas, oligodendrogliomas and oligoastrocytomas

Gene	Nucleotide change	Amino acid change	N (%)
IDH1	G395A	R132H	664 (92.7%)
	C394T	R132C	29 (4.2%)
	C394A	R132S	11 (1.5%)
	C394G	R132G	10 (1.4%)
	G395T	R132L	2 (0.2%)
IDH2	G515A	R172K	20 (64.5%)
	G515T	R172M	6 (19.3%)
	A514T	R172W	5 (16.2%)

N (%) number of tumors and percentage of mutation among all mutations

Reference: Hartmann, C., Meyer, J., Balss, J., Capper, D., Mueller, W., Christians, A., Felsberg, J., Wolter, M., Mawrin, C. & Wick, W. 2009. Type and frequency of IDH1 and IDH2 mutations are related to astrocytic and oligodendroglial differentiation and age: a study of 1,010 diffuse gliomas. *Acta neuropathologica,* 118, 469-474.

2.3.3 Role of The IDH1/IDH2 Mutations in Tumorigenesis

The wildtype IDH1 and IDH2 enzymes normally catalyze the oxidative decarboxylation of isocitrate to form αKG in the TCA cycle however, αKG is generally consumed in IDH1/2 mutated cells to generate 2-HG. The decrease in the level of αKG, an essential intermediate metabolite in the TCA cycle, cause the disruption of the TCA cycle metabolism and the glycolytic influx (Khurshed et al., 2017). In addition, αKG is not only a metabolite involved in the TCA cycle but is also used by αKG-dependent dioxygenases enzymes as a substrate for the activation of significant processes in the cell such as epigenetic regulation, DNA repair, hypoxia adaptation, and fatty-acid metabolism (Loenarz and Schofield, 2008). The pathways of these reactions related to αKG may be adversely affected due to the low amount of αKG.

While IDH1/2 wildtype enzymes provide the production of NADPH that is an important source for the reduction of reactive oxygen species (ROS), mutated IDH1/2 enzymes

convert NADPH to NADP$^+$ in the synthesis of 2HG from αKG (Molenaar et al., 2014). Hence, the level of NADP is increased rather than NADPH in IDH1/2 mutated cell, and this results in the change of the cellular NADPH/NADP$^+$ balance in cell metabolism, that induces to increase the ROS levels and also, oxidative stress. The increased oxidative stress causes DNA damage and genomic instability (Ying, 2008, Bleeker et al., 2010).

2HG enantiomers (R-, S-) is normally produced in mitochondrial metabolism (Kranendijk et al., 2012), and these unwanted products of cellular metabolism are kept at <0.1 mM as intracellular levels in normal cells by 2HG dehydrogenases (2HGDH), FAD-dependent mitochondrial enzymes (Struys et al., 2005). Mutant IDHs cause only the overproduction of (R)-2HG and the accumulation of this enantiomer. Mutant IDH-derived (R)-2HG has proven to be an oncometabolite by discovering that the cancer-associated mutant IDH1/2 gain a neomorphic enzymatic function (Dang et al., 2009). 2HG which is structurally similar to αKG binds to αKG binding site in αKG-dependent dioxygenases, and so 2HG inhibits these enzymes at least partially. Mutant IDH-derived (R)-2HG as an oncometabolite can affect epigenetic regulations and metabolism adversely by binding competitively to αKG-dependent dioxygenase enzyme family, and so it has been proposed that this oncometabolite promote cellular transformation (Xu et al., 2011).

One of the significant results of IDH1 and IDH2 mutation is definitely the change of epigenome. Deregulation of DNA methylation such as promoter CpG island hypermethylation which results in transcriptional silencing of tumor suppressor genes is associated with human cancers. In a previous study, a Glioma CpG Island Methylator Phenotype (G-CIMP) was identified by the analysis of a group of glioma samples that are patterns of hypermethylated CpG islands. In this study, It was demonstrated that the IDH1 mutation was interestingly present in these G-CIMP positive samples (Noushmehr et al., 2010). Moreover, it has been represented that IDH1/2 mutations are directly effective for the formation of this G-CIMP in another study. G-CIMP in mutant IDH1 gliomas includes the inhibition mechanism of Ten-eleven translocation (TET), which is a family of αKG-dependent dioxygenases, due to over 2HG production. 5-methylcytosine hydroxylases which are TET family members and act a role in an important step of DNA demethylation

are inhibited by binding 2HG instead of αKG, and as a result, this leads to DNA hypermethylation and the observed G-CIMP (Turcan et al., 2012).

The JmjC domain histone demethylases are another family of αKG-dependent dioxygenase enzymes which are inhibited competitively by 2HG. These regulator enzymes are essential for the regulation of chromatin conformation and gene expression appropriately (Chowdhury et al., 2011). IDH1/2 mutations impair the patterns of histone methylation, which have an effect on the expression of tumor suppressor genes, oncogenes, and metabolic genes, via the changes of DNA methylation and post-translational histone modifications. In previous studies, it was indicated that the mutated IDH1 and IDH2 enzymes in the cell can prevent cell differentiation, proliferation, metabolism, and survival, due to 2HG-dependent epigenetic alterations (Lu et al., 2012).

3. MATERIALS AND METHODS

3.1 MATERIALS

3.1.1 Plasmid

pcDNA3-Flag-IDH1 plasmid (Cat. No. 62906) which expresses wildtype IDH1 in mammalian cells was purchased from Addgene Inc. (Cambridge, MA). Also, it is known that this plasmid was previously used to study the catalytic activity of IDH1 in gliomas (Zhao et al., 2009). The map of pcDNA3-Flag-IDH1 is shown in Figure 3.1.

Figure 3.1: The map of pcDNA3-Flag-IDH1
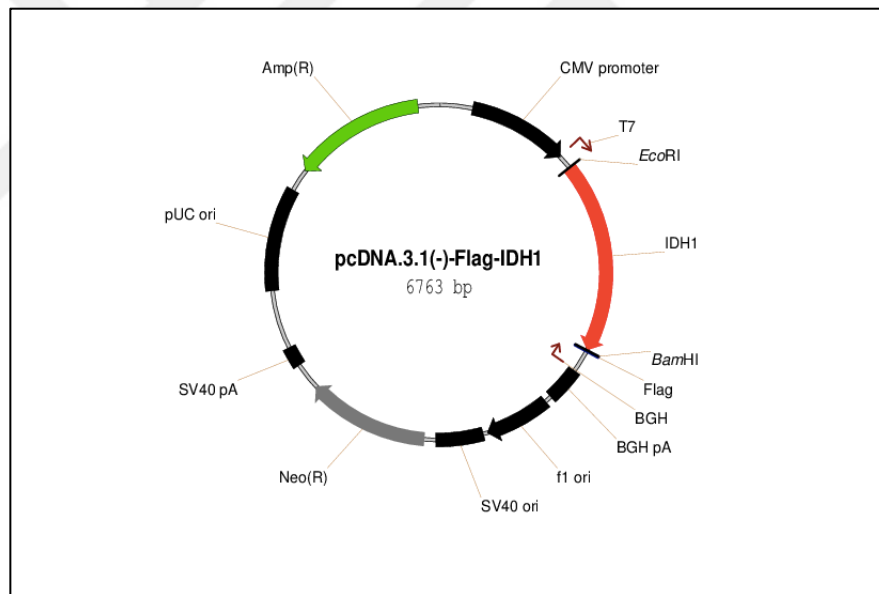
Reference: pcDNA3-Flag-IDH1. 2015. [online] https://www.addgene.org/62906/. [accessed 5 December 2018].

3.1.2 Preparation of Liquid Luria Broth (LB) Medium

Liquid LB medium used during in this study were prepared with chemicals indicated in Table 3.1. The prepared medium was autoclaved at 121°C for 20 min. The LB medium was stored at room temperature.

Table 3.1: Ingredients of liquid LB medium

Chemical	Amount
NaCl	10 g
Tryptone	10 g
Yeast extract	5 g
Water	to 1L

Reference: This table was prepared by Gizem TURAN

3.1.3 Preparation of Solid LB Plates

The preparation of solid LB medium was made with chemicals mention in Table 3.2. The medium was autoclaved at 121°C for 20 min. After cooling at 55°C, Ampicillin (Amp) or Kanamycin (Kan) antibiotic was added into LB medium by 1:1000 ratio and the medium was poured to petri dishes. These plates were stored at 4°C for a long-term storage.

Table 3.2: Ingredients of solid LB medium

Chemical	Amount
NaCl	10 g
Tryptone	10 g
Yeast extract	5 g
Agar	17 g
Water	to 1L

Reference: This table was prepared by Gizem TURAN

3.1.4 Cultivation of pcDNA3-Flag-IDH1 Plasmid, Stock Preparation and Plasmid Isolation

pcDNA3-Flag-IDH1 plasmid was sent in bacteria as 'bacterial stab' from Addgene Inc. Bacteria was inoculated with streak technique onto LB-Amp agar plate with by using 'bacterial stab' to obtain single colony. After overnight incubation at 37°C in incubator, single colonies were taken from Amp plate and inoculated in 5 mL liquid LB with 5 µL Amp. After overnight incubation at 37°C 250 rpm in shaker incubator, firstly bacteria

stock was made by mixing 350 μL 50 percent of glycerol and 500 μL bacteria culture. This mixture was stirred by vortexing and placed at -80°C for storage. Then, plasmid isolation was performed with the remaining bacteria culture by using Macherey-Nagel NucleoSpin Plasmid Kit, and plasmid DNA was kept at -20°C.

3.1.5 Chemicals, Kits, and Enzymes

All chemicals, kits and enzymes used in this study are listed in Table 3.3 and Table 3.4.

Table 3.3: List of chemicals and enzymes

Product	Trademark	Catalog No.
10X Cut Smart Buffer	NEB	B7204S
10X Phosphate Buffered Saline (PBS)	ThermoFisher	10010023
1kb Plus DNA Ladder	ThermoFisher	LSG-SM1331
6X Loading Dye	ThermoFisher	LSG-SM1331
Absolute Ethanol	Sigma-Aldrich	32221-2.5L
AflII Restriction Enzyme	NEB	R0520S
Agar Bacteriological	Scharlau	07-004-500
Agarose	BIOMAX	HS-8000
Ampicillin	AppliChem	A0839-10G
Boric acid (ortho-)	VWR	33601-261
DMEM High Glucose	WISENT	319-005CL
dNTP	NEB	N0447S
EcoRI-HF	NEB	R3101S
Ethidium bromide	VWR	0492-5G
Ethylenediaminetetraacetic acid (EDTA)	Sigma-Aldrich	EDS-500G
Fetal Bovine Serum (FBS), Heat-inactivated	ThermoFisher	10500064
Glucose (D-)	VWR	0188-1KG
Glycerol	VWR	0854-1L
Kanamycin	AppliChem	A1493.0010
NEBuilder® HiFi DNA Assembly Master Mix	NEB	E2621S

Product	Trademark	Catalog No.
Penicillin-streptomycin (P/S)	WISENT	450-201-EL
PFU Ultra II Fusion HS DNA Polymerase	Agilent	600670-51
Q5® DNA Polymerase	NEB	M0491S
Sodium chloride	Sigma-Aldrich	31434-1KG
Sterile water	WISENT	809-115-CL
Taq 2X Master Mix	NEB	M0270L
Trizma base	Sigma-Aldrich	T6066-1KG
Trypsin	Biowest	L0931-100
Tryptone	VWR	84610.05
Yeast extract	VWR	84601.05

Reference: This table was prepared by Gizem TURAN

Table 3.4: List of kits

Kit	Trademark	Catalog No.
NucleoSpin® Plasmid Kit	Macherey-Nagel	740588.50
NucleoSpin Gel and PCR Clean-up Kit	Macherey-Nagel	740609.50
Neon^{TM} Transfection System 100 μL Kit	Invitrogen	MPK10096

Reference: This table was prepared by Gizem TURAN

3.1.6 Equipment

Laboratory equipment used in this research is listed in Table 3.5.

Table 3.5: List of equipment

Equipment	Trademark
Orbital shaker incubator	Mrc, Germany
UN55 sketch universal oven	Memmert, Germay
Ultra-Low Temperature Freezer (-86)	DAIHAN Scientific, Korea
Nanopac-300 & 500 Power Supply	Cleaver Scientific, UK
ChemiDoc MP System	Bio-Rad, USA

Equipment	Trademark
Thermal cycler	Bio-Rad, USA
Vortex	Scilogex, UK
PURELAB Option-Q	ELGA, UK
Neon^{TM} Transfection System	Invitrogen, CA
Heat Block	Benchmark, USA
MicroPulser Electroporator	Bio-Rad, USA
Shaking Water Bath	DAIHAN Scientific, Korea
Microcentrifuge 16	Beckman Coulter, USA
SL 40-FR Centrifuge	Thermo Fisher, USA
T80+ UV/VIS Spectrophotometer	PG Instruments, UK
Electronic Balance	Shimadzu, JAPAN
Cell Culture Incubator	Panasonic, USA
Sub-Cell® GT Cell	Bio-Rad, USA
Leica DMIL Inverted Microscope	Leica, Germany
Leica Fluorescence Microscope	Leica, Germany

Reference: This table was prepared by Gizem TURAN

3.1.7 Sequences of Primers

Forward and reverse sequences of primers used in Gibson Assembly, Site Directed Mutagenesis (SDM) and Polymerase Chain Reaction (PCR) methods are listed in Table 3.6.

Table 3.6: List of primers

Primer	Sequence
EGFP-Fragment Forward	GTTTAAACGGTCTCCAGCTTAAGCACCATGGTGAGCAAGGGCGAG
EGFP-Fragment Reverse	CTGATCAGCGGTTTAAACTTACTTGTACAGCTCGTCCATG
CMV Forward	CGCAAATGGGCGGTAGGCGTG
BGH Reverse	TAGAAGGCACAGTCGAGG
p-IRES2-IDH1-addgene-Froward	GATCTCGAGCTCAAGCTTCGAATTCACCATGTACCCATACGATGTTCCAGATTACGCTATGTCCAAGAAAATCAGTGG
p-IRES2-IDH1-addegene Reverse	CGCGGTACCGTCGACTGCAGAATTCTTAAAGTTTGGCCTGAGCTAG
IDH1 cDNA-mut-G395A Forward	AAAACCTATCATCATAGGTCATCATGCTTATGGGGATCAAT
IDH1 cDNA-mut-G395A Reverse	ATTGATCCCCATAAGCATGATGACCTATGATGATAGGTTTT

Primer	Sequence
IDH1 cDNA-mut-G395T Forward	AAAACCTATCATCATAGGTCTTCATGCTTATGGGGATCAAT
IDH1 cDNA-mut-G395T Reverse	ATTGATCCCCATAAGCATGAAGACCTATGATGATAGGTTTT
IDH1 cDNA-mut-C394T Forward	GTAAAACCTATCATCATAGGTTGTCATGCTTATGGGGATCAAT
IDH1 cDNA-mut-C394T Reverse	ATTGATCCCCATAAGCATGACAACCTATGATGATAGGTTTTAC
IDH1 cDNA-mut-C394A Forward	GTAAAACCTATCATCATAGGTAGTCATGCTTATGGGGATCAAT
IDH1 cDNA-mut-C394A Reverse	ATTGATCCCCATAAGCATGACTACCTATGATGATAGGTTTTAC

Reference: This table was prepared by Gizem TURAN

3.2 METHODS

### 3.2.1 Cloning of EGFP in pcDNA3-IDH1-Flag Vector with Gibson Assembly

It was decided to place enhanced green fluorescent protein (EGFP) into the pcDNA3-IDH1-Flag plasmid by using Gibson Assembly method because pcDNA3-IDH1-Flag plasmid did not have any region to provide expression of EGFP or any fluorescent protein. The importance of inserting any fluorescent protein into this plasmid was to look at the efficiency of transferring the plasmid to the cells after the transfection process, which is a downstream application that was planned to be performed in the later stage of this study.

3.2.1.1 Primer design

Primers were designed as the first stage of Gibson Assembly by using NEBuilder Assembly Tool. The design of a multicistronic vector that enables the co-expression of multiple genes was required to ensure the expression of both EGFP and IDH1 gene. P2A that produce equal levels of multiple genes from the same mRNA by making 'self-cleaving' was used as 2A peptide to provide co-expression of EGFP and IDH1 gene.

During primer design, the sequence of pcDNA3-IDH1-Flag (6763 bp) was used as the vector backbone. P2A must be placed between the two mRNA sequences to be expressed and the stop codon of the gene in front of the P2A must be removed. It also planned to add the Kozak sequence and the HA tag in front of the IDH1 sequence. Because of all these, it was necessary to completely remove the IDH1 region in the pcDNA3-IDH1-Flag

plasmid. EcoRI and AflII restriction enzymes were selected both to remove the IDH1 region and to make the vector linear form. The IDH1 coding sequence containing the Kozak sequence and HA tag and EGFP sequence with the P2A sequence was added into the tool and after all that, NEBuilder Assembly Tool gave two pairs of primers. The flowchart of the primer design is shown in Figure 3.2.

Figure 3.2: The primer design of pcDNA3-IDH1-P2A-EGFP plasmid
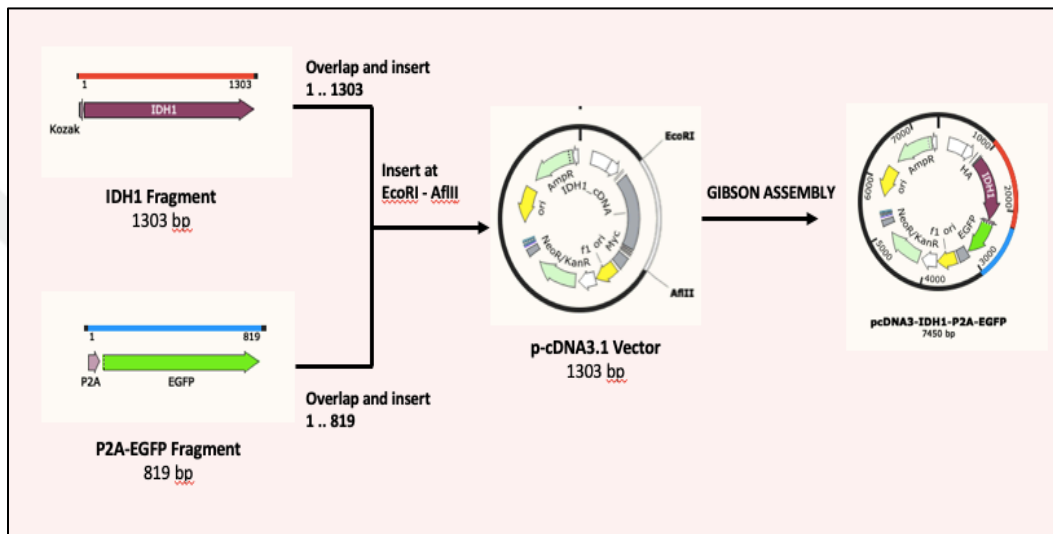
Reference: This figure was obtained from SnapGene Gibson Assembly Tool.

3.2.1.2 Amplification of target genes

IDH1 and P2A-EGFP fragments were amplified with Gibson Assembly cloning primers by PCR method to insert these fragments into pcDNA3-IDH1-Flag, IDH1 region-removed plasmid. PCR reactions applied for each insert were carried out using 1 µL plasmid DNA (5 ng/µL) p-IRES2-EGFP plasmid for EGFP and pcDNA3-IDH1-Flag plasmid for IDH1 region, 2.5 µL of Gibson cloning forward primer (10 µM), 2.5 µL of Gibson cloning reverse primer (10 µM), 1 µL of dNTP (10 mM), 10 µL NEB 5X Q5 reaction buffer, 0.5 µL NEB Q5 DNA polymerase, and 32.5 mL sterile water. PCR tubes were placed in T100 thermal cycler to run the reaction, and also PCR thermal cycler conditions are indicated in Table 3.7.

Table 3.7: PCR conditions for IDH1 and P2A-EGFP amplification

Reaction step	Temperature	Duration	Number of cycle
Initial denaturation	98°C	30 sec	1
Denaturation	98°C	10 sec	
Annealing	72°C	25 sec	35
Extension	72°C	1 min	
Final extension	72°C	2 min	1
Hold	4°C	∞	

Reference: This table was prepared by Gizem TURAN

After the PCR reaction, the PCR products were loaded to 1 percent of agarose gel, and agarose gel electrophoresis was applied at 145 volts for 80 min.

After electrophoresis analysis, IDH1 and P2A-EGFP products were cut from the agarose gel, and then the purification process was accomplished for these gel slices in order to obtain specific amplification products and get rid of primer-dimers.

3.2.1.3 Digestion of vector

To insert IDH1 and P2A-EGFP fragments into plasmid, it was decided to make the vector linear with the restriction enzyme instead of using PCR method. It was also needed to be removed IDH1 region not include Kozak sequence and HA tag from the vector backbone, the pcDNA3-IDH1-Flag. For these two purposes, EcoRI and AflII restriction enzymes were used and ultimately the IDH1 region in the pcDNA3-IDH1-Flag plasmid was completely excised with EcoRI and AflII restriction enzymes, and so the vector was also linearized.

For this digestion, 3.5 µL pcDNA3-IDH1-Flag plasmid DNA (650 ng/µL), 5 µL 10X Cut-Smart buffer, 1 µL AflII restriction enzyme, 1 µL EcoRI restriction enzyme and 39.5 µL sterile water were composed and then, this mixture was incubated at 37°C in water bath for 4 hours. After incubation, the reaction tube was put into on ice to deactivate the activation of restriction enzyme.

According to Gibson Assembly instruction manual, if there is no the same restriction region in insert DNA, the purification of the digested vector is not necessary. However, in this study, the digested vector was cut from the agarose gel after gel electrophoresis and was purified with Macherey-Nagel Gel and PCR Clean-up Kit to remove the IDH1 region, restriction enzymes and Cut-Smart buffer used in the cutting process because these components could affect Gibson Assembly reaction, which was the next step in this study.

3.2.1.4 Gibson assembly

To assemble restriction digested vector and PCR-amplified inserts, it is recommended that using a total of 0.03-0.2 pmols of DNA fragments and 1:2 (vector:insert) ratio as DNA molar ratio in NEB Gibson Assembly manual instructions. The concentration of IDH1 fragment, P2A-EGFP fragment and linearized vector (pcDNA3-IDH1-Flag, IDH1-region removed) were determined using agarose gel electrophoresis. For this aim, purified IDH1 product, P2A-EGFP product, and purified digested vector were loaded on the 1 percent of agarose gel in certain amounts as 1 µL, 2 µL, and 3 µL. 2.275 µg/µL vector was used for digestion process and after purification, it was eluted in 30 µL elution buffer so the last concentration of the vector became 75.83 ng/µL. Because the vector concentration was known, after electrophoresis, the brightness of insert fragments in the gel image was compared to the vector brightness to estimate the mass of inserts. As a result, the concentrations of insert fragments were calculated as 160 ng/µL for IDH1 fragment and 80 ng/µL for P2A-EGFP fragment. In addition, 50 ng/µL vector was used for 10 µL assembly reaction because it was indicated in the protocol. Since the 1:2 ratio was recommended, the difference between the length of vector and inserts were based on and 25 ng/µL IDH1 insert fragment and 15.4 ng/µl P2A-EGFP insert fragment were added in the reaction.

In order to set up assembly reaction, digested pcDNA3-IDH1-Flag vector, IDH1 product, P2A-EGFP product, and NEBuilder® HiFi DNA Assembly Master Mix was mixed gently on the ice and the sample was incubated in the thermal cycler at 50°C for 60 min.

Following incubation, the reaction tube was placed on ice until the subsequent step, electroporation.

The assembly product was transfected into electrocompetent cells by electroporation method to provide transformation of competent cells for reproducing this assembly product in the bacteria. Top10, a strain of *E. coli* was preferred as an electrocompetent cell.

1 µL the assembly product was added to 40 µL electrocompetent Top10 cells and mixed gently and then, this mixture was immediately put into an electroporation cuvette. After that, 1800 volt was applied to the sample with Micropulser® electroporator, and 1 mL SOC medium, a nutrient-rich medium, was given directly to competent cells. Bacteria was placed for incubation in a shaker incubator at 37°C 250 rpm for 30 min. After all, 150 µL of the cells were inoculated onto LB-Amp agar plate with the spread technique and incubated overnight at 37°C.

To find out whether the colonies growing in the LB-Amp plates contained the desired targets, IDH1 and P2A-EGFP, colony PCR was performed. Colonies were taken from Amp agar plate by using pipette tip, and this pipette tip was first put into the bottom of the PCR tubes to leave bacterial DNA into the tubes, then the tip was applied on another LB-Amp agar plate to form the colony. For each PCR reaction tube, 1 µL Gibson Cloning forward primer, 1 µL Gibson Cloning reverse primer, 10 µL NEB Taq 2X Master Mix, and 8 µL sterile water were mixed, and also tubes were placed in T100 thermal cycler. PCR thermal cycler conditions are indicated in Table 3.8. Besides, the newly prepared Amp plate was incubated overnight at 37°C.

Table 3.8: Thermal cycler conditions of colony PCR

Reaction step	Temperature	Duration	Number of cycle
Initial denaturation	95°C	3 min	1
Denaturation	95°C	30 sec	
Annealing	50°C	30 sec	37

Reaction step	Temperature	Duration	Number of cycle
Extension	72°C	1 min 15 sec	37
Final extension	72°C	5 min	1
Hold	4°C	∞	

Reference: This table was prepared by Gizem TURAN

After gel electrophoreses with 1 percent of agarose gel, the selected samples were sequenced with Sanger sequencing method by using Gibson Cloning primers.

### 3.2.2 Cloning of IDH1 in p-IRES2-EGFP Vector with Gibson Assembly

In parallel with our multicistronic vector design, pcDNA3-IDH1-P2A-EGFP, it was decided to insert the desired IDH1 coding sequence to another vector containing already EGFP and the IRES (Internal Ribosome Entry Site) element which allows for initiation of translation from an internal region of the mRNA. p-IRES2-EGFP vector was chosen in accordance with this purpose.

3.2.2.1 Primer design

Since the cDNA sequence of IDH1 had to be inserted into the p-IRES2-EGFP plasmid, the Gibson Cloning primers were designed primarily. In this primer design, the sequence of p-IRES2-EGFP vector (5308 bp) was introduced into NEBuilder Assembly Tool as a vector backbone, and EcoRI restriction enzyme was chosen to cut the vector. Also, the primer design was made by adding the HA tag and Kozak sequence in front of the coding sequence of IDH1. The flow diagram of the primer design is shown in Figure 3.3.

Figure 3.3: The primer design of p-IRES2-IDH1-EGFP plasmid
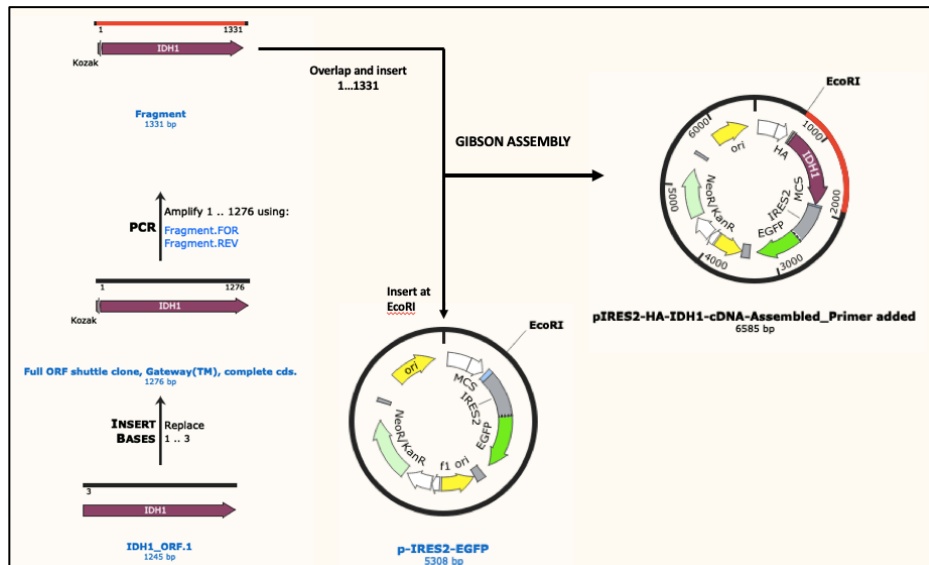
Reference: This figure was obtained from SnapGene Gibson Assembly Tool.

3.2.2.2 Preparation of fragments and Gibson assembly process

To amplify IDH1 cDNA, the pcDNA3-IDH1-Flag plasmid was used as template. PCR was performed with Gibson Cloning primers. PCR conditions were the same as before, but Thermal cycler conditions were different because the annealing temperature was 65°C at this time. For the linearization of p-IRES2-EGFP vector, 2.56 µg/µL vector was digested with EcoRI restriction enzyme same as before.

Before Gibson Assembly reaction, the concentrations of vector and insert was calculated by using the image of agarose gel electrophoresis. According to the calculation, the concentrations of vector and insert were 85 ng/µL and 28 ng/µL, respectively. The digested vector, the purified IDH1 product, sterile water, and NEBuilder® HiFi DNA Assembly Master Mix were added into a PCR tube on ice and mixed gently. The reaction product prepared was incubated in Thermal cycler at 50°C for 60 min. After the assembly reaction, 1 µL the assembly product was electroporated into Top10 electrocompetent cells. Then, bacteria were inoculated LB-Kan agar plate and incubated in incubator overnight at 37°C. After Colony PCR, the selected colonies were inoculated in liquid LB medium, and then plasmid extraction was made for the Sanger sequencing with Gibson cloning primers.

3.2.3 Site Directed Mutagenesis

Since the main purpose of this study was to observe the phenotypic effects of the different sites of IDH1 mutations, point mutations were formed in both pcDNA3-IDH1-P2A-EGFP and p-IRES2-IDH1-EGFP plasmids by site-directed mutagenesis method.

Agilent QuickChange Primer Design tool was used to design the mutagenesis primers for G395A, G395T, C394A, and C394T mutation sites of the IDH1 gene. Also, after sanger sequences analysis, p-IRES2-IDH1-EGFP 2nd and pcDNA3-IDH1-P2A-EGFP 6th colony plasmids were chosen to continue the study. To set up Mutant Strand Synthesis Reaction, 1 µL plasmid DNA (20 ng/µL), 0.5 µL forward primer (10 µM), 0.5 µL reverse primer (10 µM), 0.5 µL dNTP (10 mM), 2.5 µL 10X Pfu Reaction Buffer, 19.5 µL sterile water, and 0.5 µL Agilent PfuUltra High-Fidelity DNA polymerase were mixed on ice, and this reaction was applied to all the desired mutation points for the two plasmids. The thermal cycler conditions of this reaction were as follows: 95°C for 30 sec during 1 cycle, and 95°C for 30 sec, 55°C for 1 min, 68°C for 6 min during 16 cycles.

To generate the methylation specific digestion of the IDH1 wildtype template DNA, DPNI digestion was carried out after the Mutant Strand Synthesis Reaction. 25 µL the reaction product DNA, 5 µL 5X Cut Smart Buffer, 19 µL sterile water and 1 µL DPNI restriction enzyme were used for each reaction. The samples were kept overnight in a water bath at 37°C, and then purification was made to remove the remaining after digestion. These mutagenesis plasmids were transferred into bacteria cells by electroporation. Colonies obtained from LB-Kan agar plates after electroporation were inoculated in liquid LB medium and prepared to Sanger sequencing.

3.2.4 Mammalian Cell Transfection

To investigate the phenotype effects of mutations in the active sites of IDH1 enzyme in this study, it was planned to provide the expression of IDH1 encoding gene in mammalian cells. So that, mammalian cells transfection experiment was performed with the IDH1 wildtype and IDH1 mutations plasmids, after the sequence results of the mutagenesis

samples were obtained. Since DNA concentrations of pcDNA3-IDH1wt-P2A-EGFP and IDH1mut plasmids were low, phenotype assays were started with p-IRES2-IDH1wt-EGFP and IDH1mut plasmids.

For mammalian cell transfection with p-IRES2-IDH1wt-EGFP and four different IDH1 mutation forms of this plasmid, electroporation was performed as a transfection method using Neon Transfection System. In this study, U87MG glioma cells and non-glial 293T cells were used to observe how phenotypic differences would occur between glial and non-glial cells.

For this transfection experiment, U87-MG and 293T cells were firstly thawed by removing from the liquid nitrogen tank, and the experiment was started with healthy cells after passing two passages. U87-MG and 293T cells were washed with PBS, and after harvesting with trypsin, DMEM High Glucose supplemented with 10 percent of FBS and 1 percent of P/S was added on cells. Then, cells were counted with a hemocytometer. It was decided to transfect 3×10^6 cells for each cell line because this number was the total number of cells required for MTT Cell Viability Assay and Scratch Repair Assay after transfection. After this number of cells were taken into Eppendorf tubes, centrifugation was applied at 200 g 5 min. After that, the supernatant was removed, and cells were washed with 1 mL PBS. This step was repeated, and then the cell pellet was resuspended with Resuspension Buffer found in Neon^{TM} Transfection System 100 µL Kit. 100 µL of cells resuspended was put into Eppendorf tubes for each experimental group, and also 10 µl plasmids were distributed to each experimental group. 1300 volt, 30 ms, 1pulse electroporation for U87MG cells and 1100 volt, 20 ms, 2 pulses electroporation for 293T cells was performed by using Neon Transfection System. After DMEM High Glucose medium containing only 10 percent of FBS was immediately added onto transfected cells. The transfected cells were put into wells according to the numbers appropriate for MTT Cell Viability Assay and Scratch Repair Assay plans and then plates were placed into the incubator at 37°C with 5 percent of CO_2.

After mammalian cell transfection with p-IRES plasmids, EGFP fluorescence in U87MG glioma cells was not observed. Western Blot assay with total protein extraction from

transfected U87MG cells using the HA tag antibody revealed that the plasmids were transferred to U87MG cells due to the presence of HA tag proteins, but because of the absence of EGFP fluorescence, the expression of the EGFP protein was thought to be unrealized in these U87MG cells. It was concluded that the IRES element did not provide the expression of EGFP after the production of the IDH1 protein. Therefore, it was decided to repeat the experiments with P2A-containing pcDNA3-IDH1wt-P2A-EGFP and IDH1mut plasmids.

For mammalian cell transfection with pcDNA3-IDH1wt-P2A-EGFP and four different IDH1 mutation forms of this plasmid, PEI chemical transfection was performed as a transfection method. For this study, U87MG glioma cells and non-glial HCT cells instead of non-glial 293T cells because of the loose feature of 293T cells were used to observe how phenotypic differences would occur between glial and non-glial cells.

To perform PEI transfection, 1.75×10^6 U87MG cells and 3×10^6 HCT cells were seeded into 100 mm cell culture dishes. After two days incubation for U87MG cells and one-day incubation for HCT cells in the incubator at 37°C with 5 percent of CO_2, PEI-DNA mixture was applied to the cells. The mixture was prepared in a ratio of 1 to 3. That is, 22,5 μg PEI (1 mg/ml) and 7,5 μg plasmid DNA was mixed in 500 μl only DMEM medium. After this mixture was incubated at room temperature for 15 minutes, the media of the cells was first replaced with fresh completed medium and this mixture was given dropwise to the cells. The cells were then placed into the incubator at 37°C with 5 percent of CO_2 and harvested for the next day for MTT Cell Viability Assay and Scratch Repair Assay.

3.2.5 MTT Cell Viability Assay

To understand the effects of IDH1 mutations on cell proliferation, MTT (3-(4,5-dimethylthiazol-2-yl)-2,5-diphenyltetrazolium bromide) Cell Viability Assay was carried out. 2.0×10^4 U87MG and 293T cells transfected with Neon Transfection method and 2.0×10^4 U87MG and HCT cells transfected with PEI chemical were seeded into 24-well plates. The next day, for cell viability analysis, 50μl MTT (5mg/ml in PBS) was added to

each well and incubated for 4 hours into the incubator at 37°C with 5 percent of CO_2. 500 μl SDS solubilization buffer (0.1 M HCl 10% SDS) was used to solubilize formazan crystals and cells incubated for 15 minutes at 37°C. The absorbances were measured by spectrophotometer at 570nm. Also, this experiment was carried out for 5 days.

Since MTT assay was performed for 5 days, the cells were examined with a fluorescence microscope for 5 days as it was necessary to confirm that the plasmids were present in the cells during this period. Therefore, approximately 3.0×10^5 transfected cells were seeded into 6-well plates and images were taken every day with fluorescence microscopy.

3.2.6 Scratch Repair Assay

To investigate the effects of IDH1 mutations on cell migration, it was planned that scratch repair assay was performed. In this assay, 293T cell line was not used because this cell line has a very loose structure and after making the wound, they have a tendency to detach from the plate immediately. For this assay, 2.5×10^5 transfected U87MG cells and 3.0×10^5 transfected HCT were planted in each well of 12-well plate and incubated in the incubator at 37°C with 5 percent of CO_2. After the cells hold onto the surface and complete their morphological forms, a straight-line scratch was applied on confluent cells by using a sterile 1000 μL pipette tip. Then, the fresh 1 mL DMEM High Glucose supplemented with 10 percent of FBS and 1 percent of P/S was added. Images were taken at 0, 8, 24 hours for the experiment making with U87MG transfected by Neon Transfection and at 0, 24, 48, and 72 hours for transfected U87MG and HCT cells

3.2.7 Western Blot

To confirm whether the IDH1 coding gene in our plasmid was expressed in the mammalian cells after mammalian cell transfection, Western Blot assay was carried out. In this assay, we attempted to detect the IDH1 protein using the antibody of the HA tag located in front of the IDH1sequence in our plasmid.

Prior to the Western Blot experiment, protein extraction from transfected cells was performed with G-Biosciences Total Protein Extraction Kit. In the protein extraction method, firstly cells were washed at least three times with PBS and then, PBS was added again after washing and cells were scraped out of dishes. Cells in PBS were collected in the falcon tubes and centrifuged at 250 g for 5 min. After centrifugation, the pellet was resuspended with 400 µL TBE buffer I supplemented with protease inhibitor cocktail and the resuspended sample was incubated on the ice for 2 min. After that, 240 µL TBE buffer II was added and the sample was heated in boiling water for 30 sec. The sample was vortexed for 30 seconds and put into boiling water again for 10 minutes. Finally, centrifugation was done at 1300 g for 5 min to remove non-protein artifacts and supernatants were transferred to new tubes.

For Western Blot assay, 30 µg cell lysates were loaded into 8-15% SDS polyacrylamide gel and electrophoresis was performed until bromophenol blue dye run out from the gel. Proteins were transferred to 0.45µm pored sized nitrocellulose membrane with wet transfer conditions; 90 volts 100 minutes. Samples were transferred to 0.45µm pored sized nitrocellulose membrane with wet transfer methods. After the transfer process, blocking was applied with %5 non-fat powdered milk in TBST at room temperature for an hour. Then, 4ml of 1:1000 diluted HA-Tag and Actin antibodies in 5% non-fat powdered milk were introduced into membranes for overnight incubation at 4°C. The next day, membranes were washed four times with TBST. After that, secondary antibodies were 1:10000 diluted and they were introduced into membranes for 1 hour at room temperature. After four TBST washes again, the target of proteins' reactivity was developed by hydrogen-peroxide chemiluminescence according to the manufacturer's instructions.

4. RESULTS AND DISCUSSION

4.1 GENERATION OF pcDNA3-IDH1-P2A-EGFP AND p-IRES2-IDH1-EGFP CONSTRUCTS

To detect whether the colonies obtained after Gibson assembly included the IDH1 fragment, colony PCR was applied by using Gibson assembly cloning primers. The result of agarose gel electrophoresis of colony PCR is represented in Figure 4.2. As seen in the gel image, it was observed that IDH1 coding region was found in all colonies obtained.

Figure 4.1: The colony PCR result of pcDNA3-IDH1-P2A-EGFP
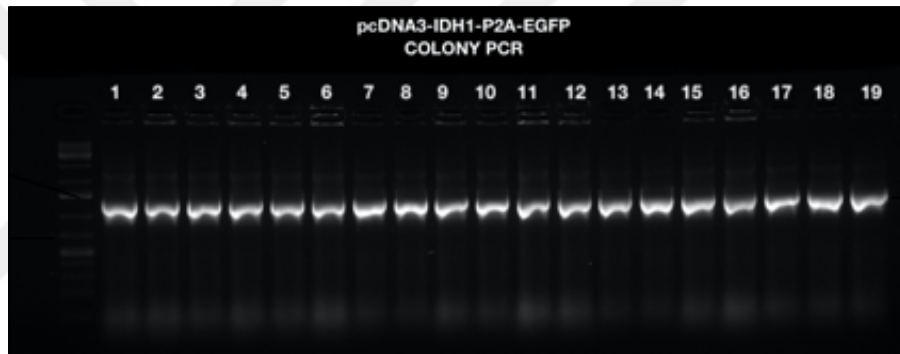
Reference: This photograph was taken by Gizem TURAN

Sanger sequencing was applied to our plasmid DNA in addition to Colony PCR to confirm that the plasmid construct was correctly generated. Sanger sequence result was aligned in SnapGene tool and as shown in Figure 4.2 the red line indicates the sequence region. As a result, the IDH1 coding sequence was completely transferred into the pcDNA3 vector backbone.

Figure 4.2: Sanger sequencing result of pcDNA3-IDH1-P2A-EGFP construct
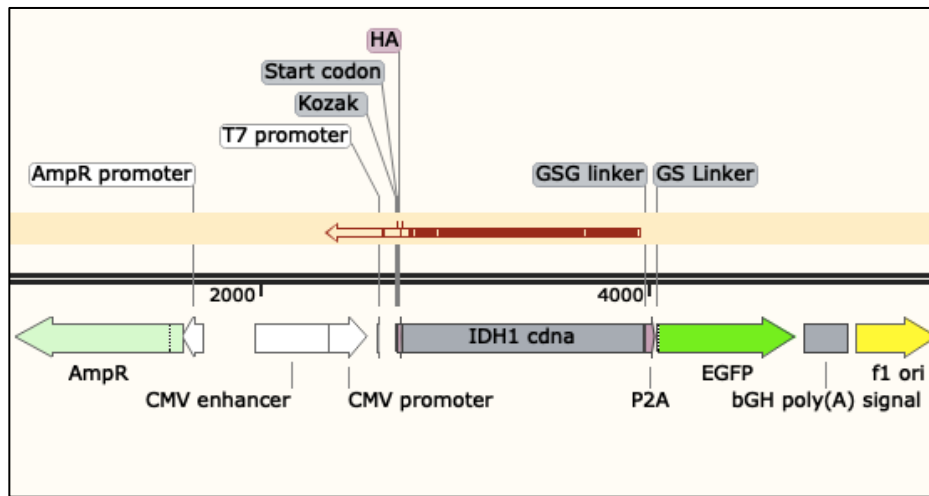
Likewise, both Colony PCR and Sanger sequencing were performed in the other plasmid construct, p-IRES2-IDH1-EGFP. Colony PCR gel image given in Figure 4.3 shows that this construct also contains the IDH1 region. Also, the IDH1 insertion into p-IRES2-EGFP vector was also confirmed by Sanger sequencing as shown in Figure 4.4.
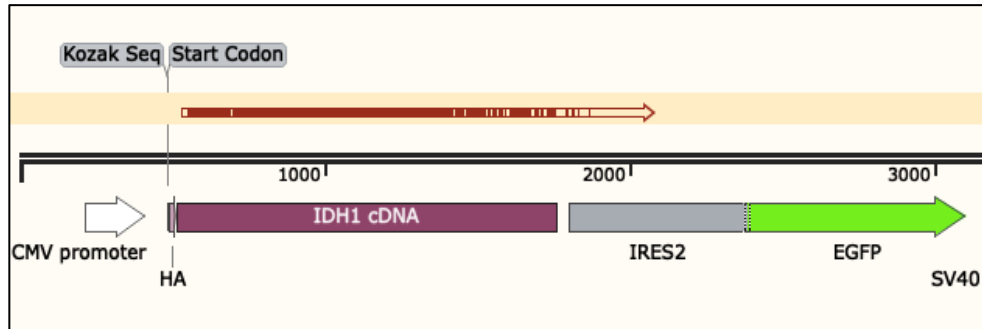
Figure 4.3: The colony PCR result of p-IRES2-IDH1-EGFP
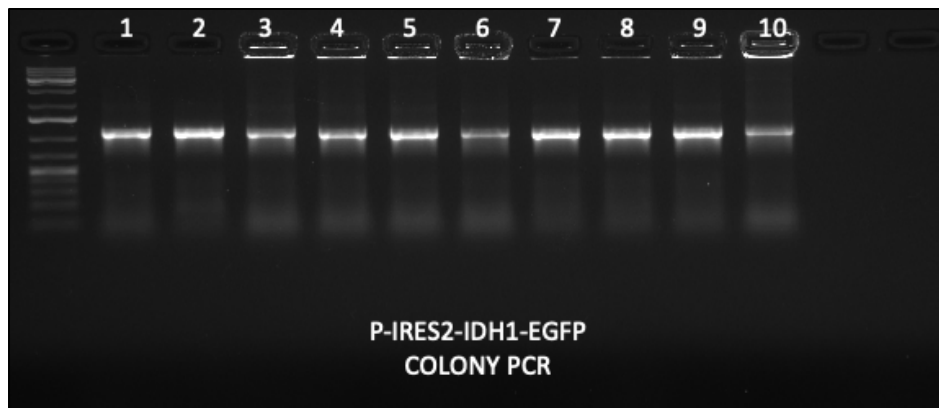
Figure 4.4: Sanger sequencing result of p-IRES2-IDH1-EGFP construct

Reference: This photograph was taken by Gizem TURAN

4.2 CREATION OF MUTANT DNA CONSTRUCTS

The primary purpose of this study was to examine the phenotypic effects of four different IDH1 mutations on cells and was perhaps to determine their role in tumor formation. Therefore, the four different point mutations containing the G395A, G395T, C394A, C394T nucleotide changes as was formed in both pcDNA3-IDH1-P2A-EGFP and p-IRES2-IDH1-EGFP plasmids by site-directed mutagenesis method. In both plasmids containing IDH1 wildtype coding sequence, these four mutations were successfully generated, and in Figure 4.5 the Sanger results of these mutations were given. In the figures showing the results of the sequencing, the red arrows indicate the peaks of the nucleotides modified as mutants.

**Figure 4.5: Sanger sequencing result of mutant DNA constructs**

Reference: This photograph was taken by Gizem TURAN

36
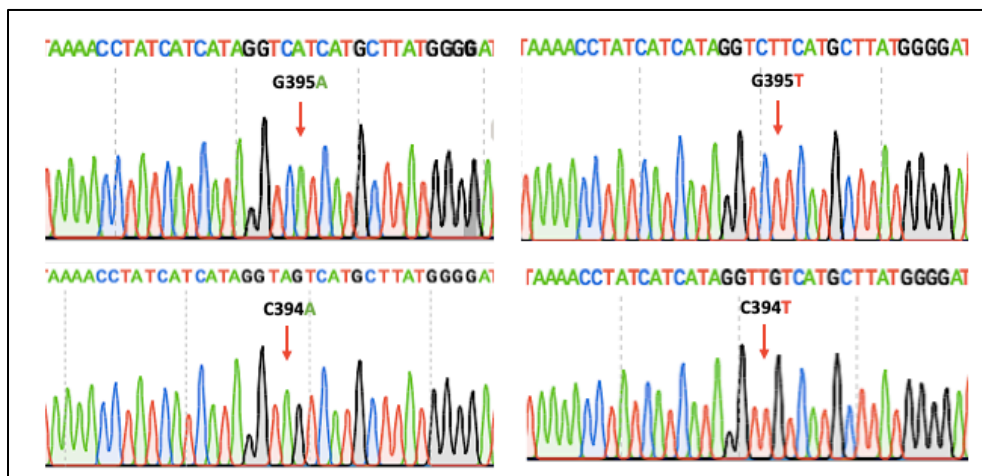
4.3 CELL VIABILITY ANALYSIS OF CELLS TRANSFECTED WITH IDH1^{WT} AND IDH1^{MUT} DNA CONSTRUCTS

To investigate the effects of IDH1 mutations on cell proliferation, firstly, p-IRES2-IDH1-EGFP plasmids including IDH1 wildtype (IDH1^{WT}) and IDH1 mutant (IDH1^{MUT}) sequence were transfected into non-glial 293T cells and U87MG glioma cells by electroporation method, and after MTT Cell Viability assay was performed for 5 days.

MTT results from 293T are shown in Figure 4.6. Furthermore, both phase contrast images and fluorescence images of the cells were taken throughout this experiment, i.e. for 5 days (Figure 4.7 and Figure 4.8). According to MTT result graphs, except G395A mutation, IDH1 mutations decrease cell proliferation compared to the control and IDH1-WT groups in 293T cells. In fact, this reduction is observed in C394T mutation more than the others. The G395A mutation showed similar results to the control and IDH1-WT groups, and this mutation did not cause any change in this cell line upon cell proliferation.
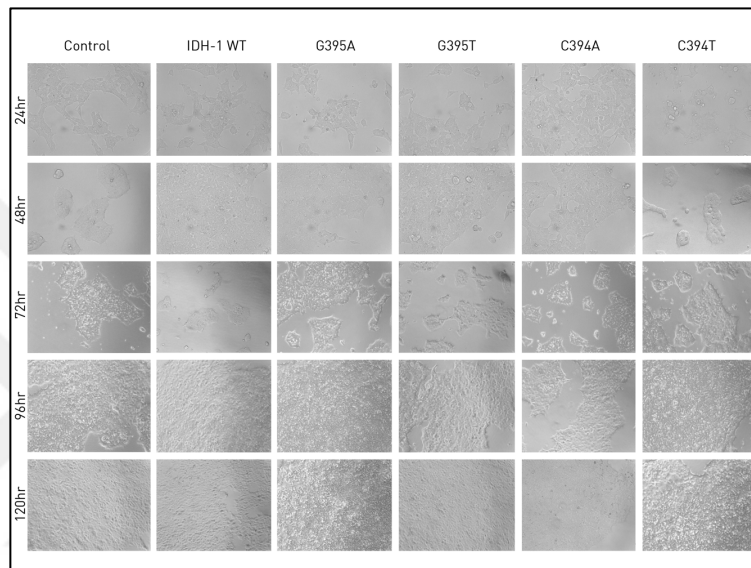
Figure 4.6: The results of MTT cell viability assay with 293T cells

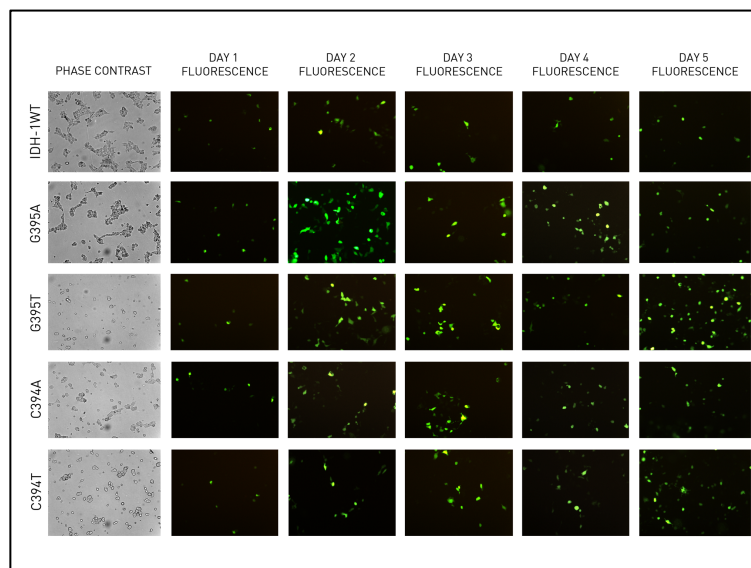*Reference:* This photograph was taken by Gizem TURAN

37
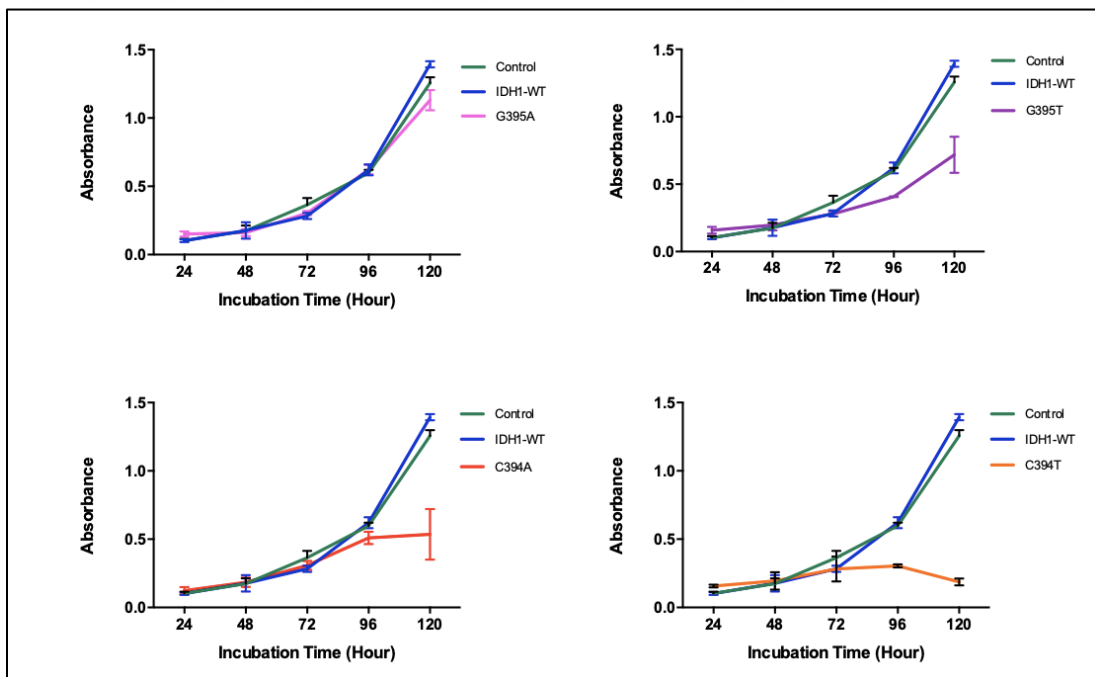
As seen in the phase contrast images of the cells, the cells throughout the MTT assay were seen as healthy by preserving their morphology. In addition, fluorescence images taken for 5 days show that our plasmids were in the cells and were expressed by these mammalian cells during MTT assay. This gives the right to interpret MTT analysis within the framework of these mutations.

Figure 4.7: The images of 293T cells during MTT assay

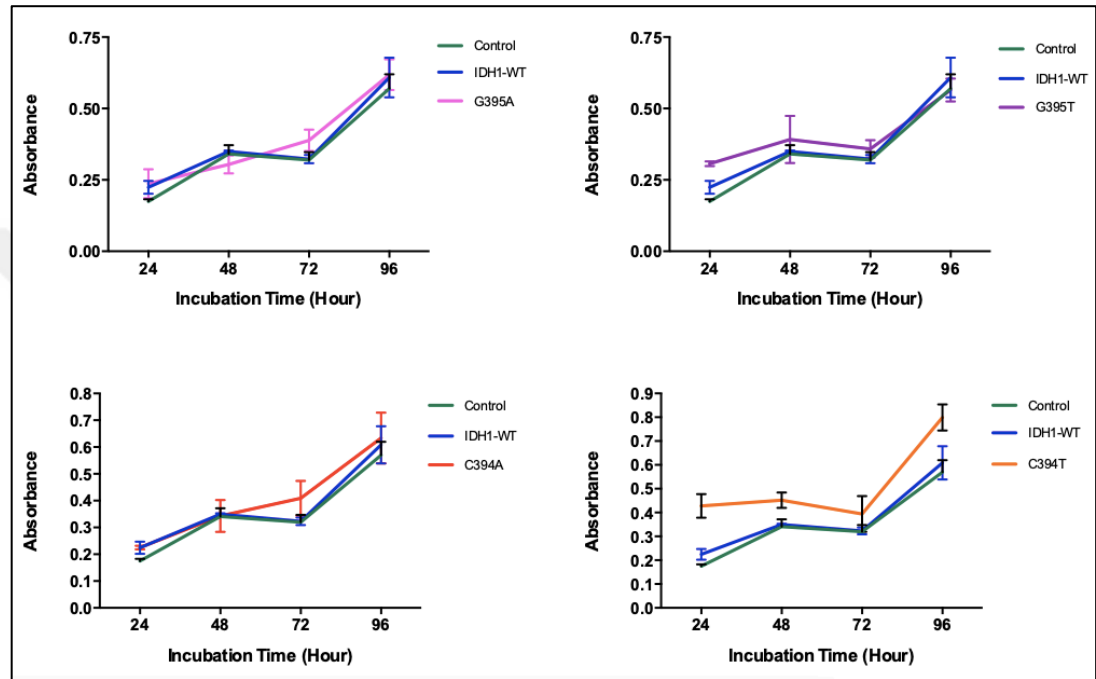
Reference: This photograph was taken by Gizem TURAN

Figure 4.8: The fluorescence images of 293T cells transfected during MTT assay

Reference: This photograph was taken by Gizem TURAN

The analysis of the MTT assay in U87MG cells was performed for four days without including the 5th day because of the increased variation in the absorbance results obtained on the 5th day. As shown in Figure 4.9, IDH1 mutations have no effect on cell proliferation in U87MG glioma cells.

Figure 4.9: The results of MTT cell viability assay with U87MG cells

Reference: This photograph was taken by Gizem TURAN

In the U87MG phase contrast images given in Figure 4.10, cells are observed in healthy structures. GFP fluorescence was not seen in these cells for 5 days, but these MTT results can be interpreted because the presence of plasmids in these cells was demonstrated by Western Blot assay (Western Blot results are at the end of the result section).

**Figure 4.10: The images of U87MG cells during MTT assay**
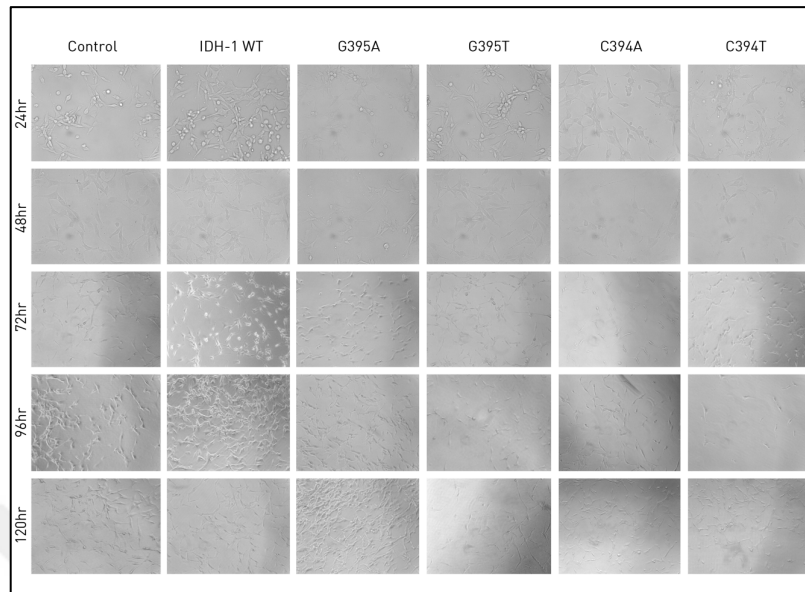
The reason for the absence of GFP fluorescence was thought to be that the IRES element in the plasmid did not fulfill its function. Therefore, experiments were repeated with pcDNA3-IDH1-P2A-EGFP plasmids including IDH1 wildtype (IDH1^{WT}) and IDH1 mutant (IDH1^{MUT}) because P2A peptide is better able to perform co-expression than IRES element. These plasmids were transfected into non-glial HCT cells and U87MG glioma cells by PEI chemical method, and after MTT Cell Viability assay was performed for 5 days.

MTT results of HCT cells are given in Figure 4.11. According to MTT result graphs of HCT, it is seen that C394T mutation decrease cell proliferation compared to the control and IDH1-WT groups in HCT cells. Also, the other IDH1 mutations have no effect on cell proliferation.
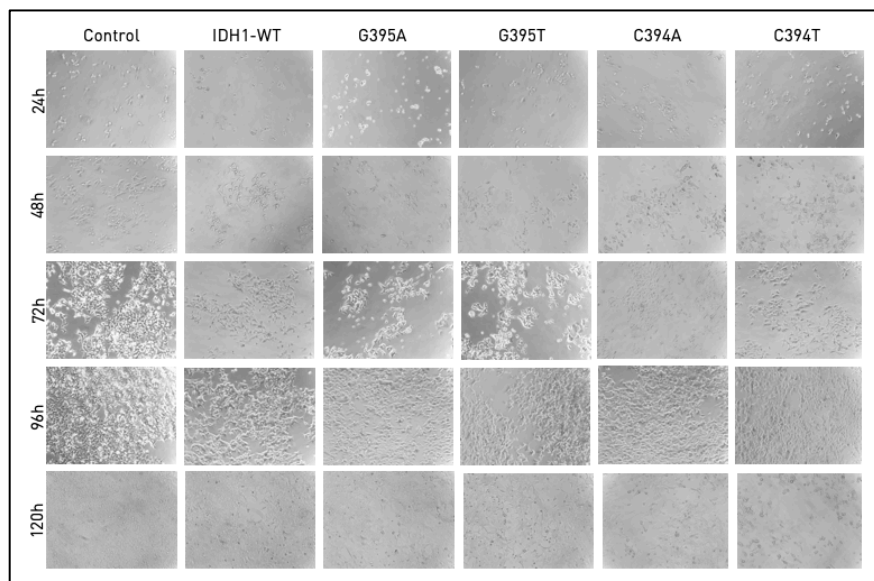
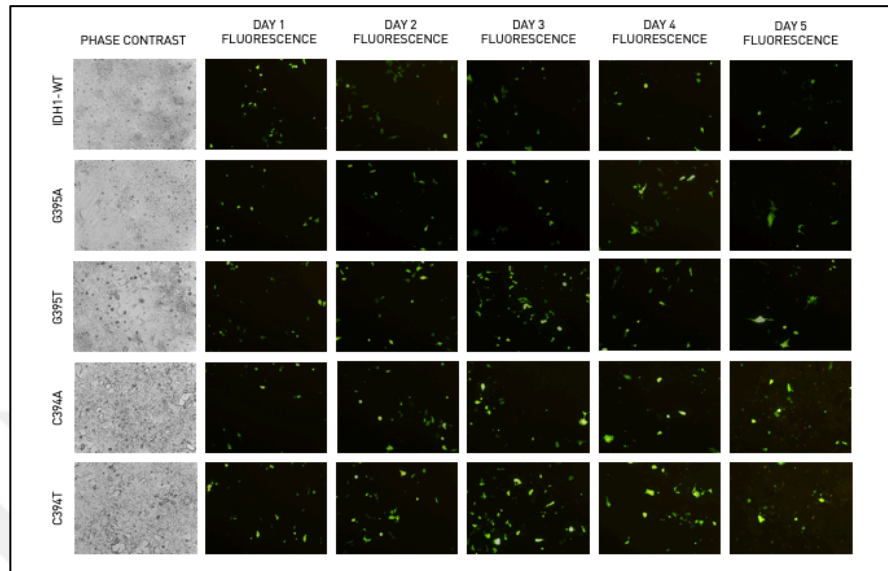**Figure 4.11: The results of MTT cell viability assay with HCT cells**
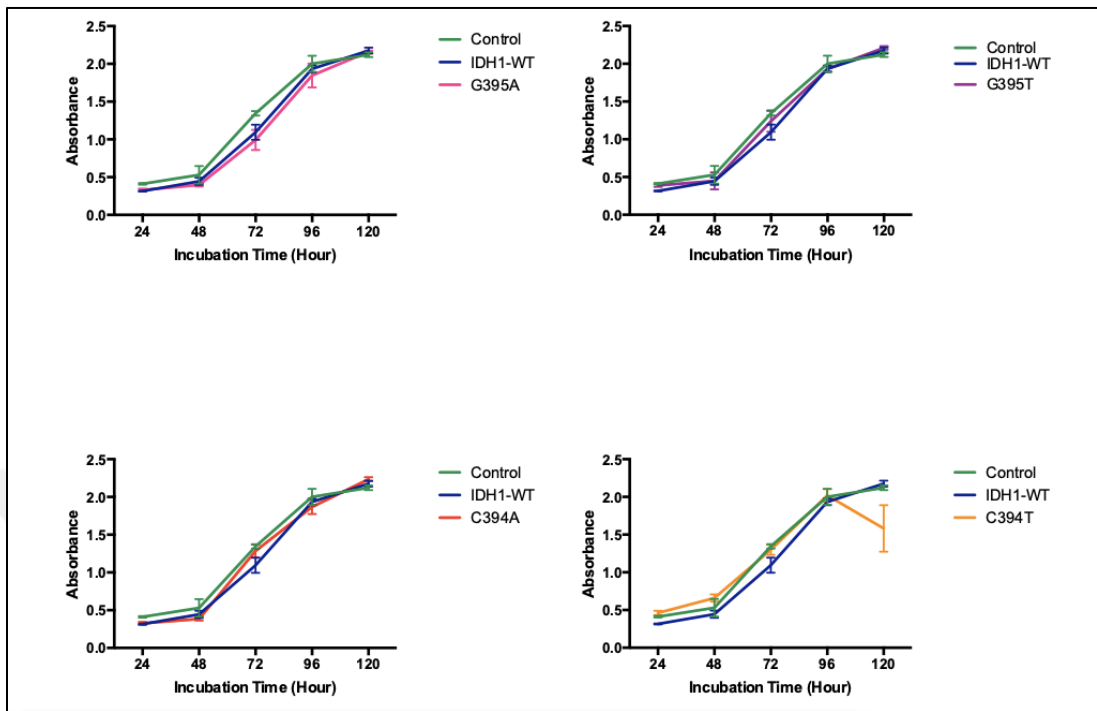
The phase contrast images of HCT transfected cells are given in Figure 4.12 and the fluorescence images of these cells are shown in Figure 4.13.

Figure 4.12: The phase contrast images of HCT cells during MTT assay

Figure 4.13: The fluorescence images of HCT cells transfected during MTT assay

When compared to the fluorescence images of 293T cells with images of HCT cells, it can be seen that transfection efficiency in HCT cells, which transfected by PEI chemical transfection method, is more than 293T cells transfected by electroporation method.

The graphs of MTT analysis, the phase contrast images and fluorescence images of U87MG cells transfected by PEI transfection method are shown in Figure 14, 15, and 16, respectively. According to MTT results, when compared to the control group, both wildtype and mutation groups were observed to have less cell viability. In fact, when the phase contrast images of the cells are examined, it is seen that most of the cells after transfection died from PEI chemical. PEI created a toxic effect for U87MG cells, and so the morphological structures of the cells were impaired. As a result, MTT results cannot be considered as an effect of mutations because transfection did not occur successfully. Furthermore, when the fluorescence images were examined, it was observed that the transfection efficiency was quite low in these cells.

Figure 4.14: The results of MTT cell viability assay with U87MG cells transfected with PEI

Reference: This photograph was taken by Gizem TURAN

Figure 4.15: The phase contrast images of U87MG cells during MTT assay

Reference: This photograph was taken by Gizem TURAN

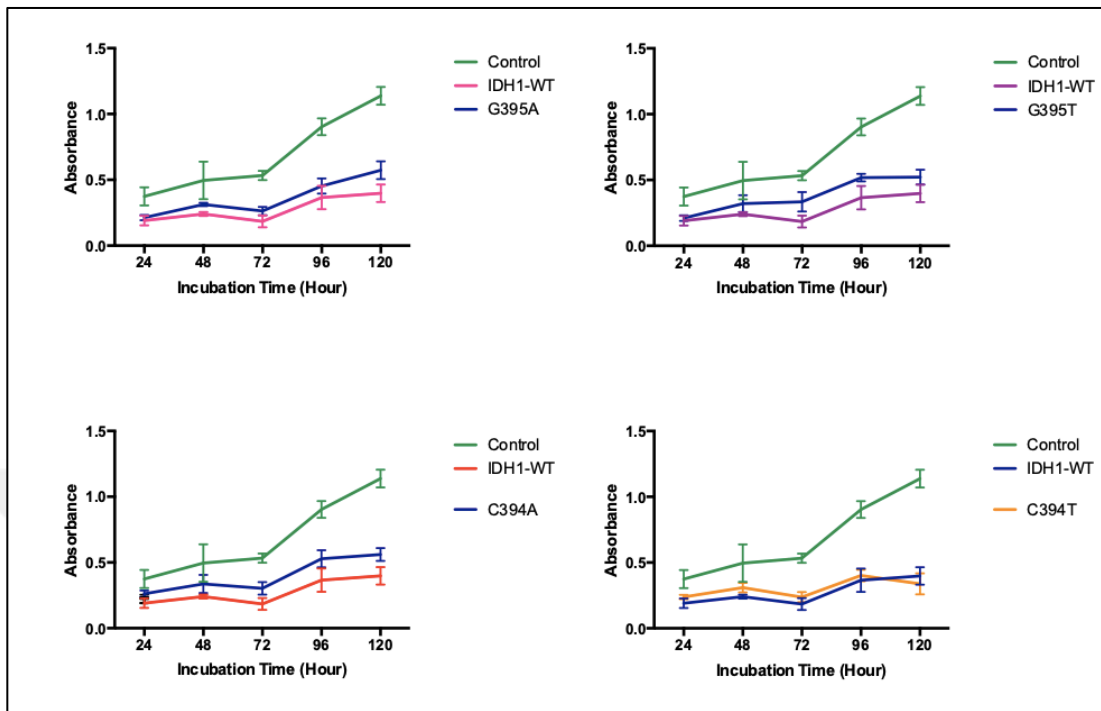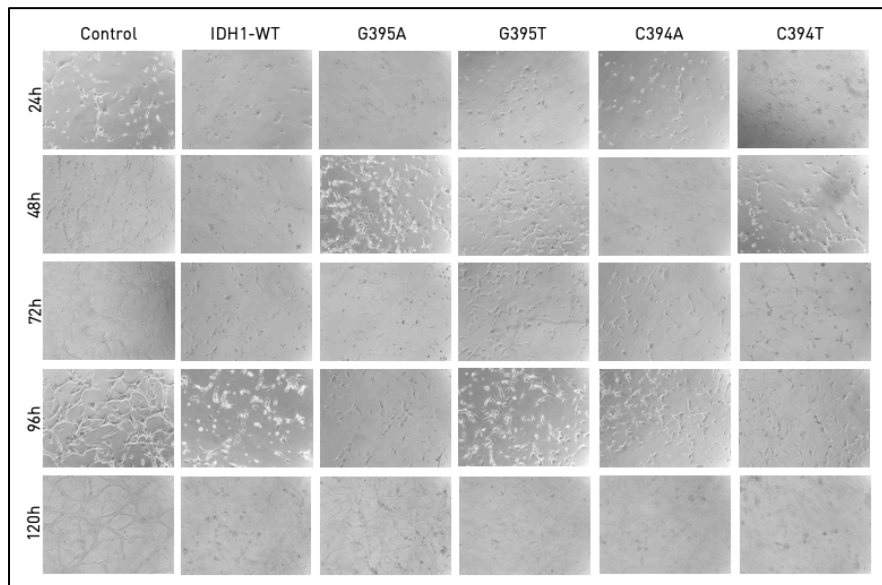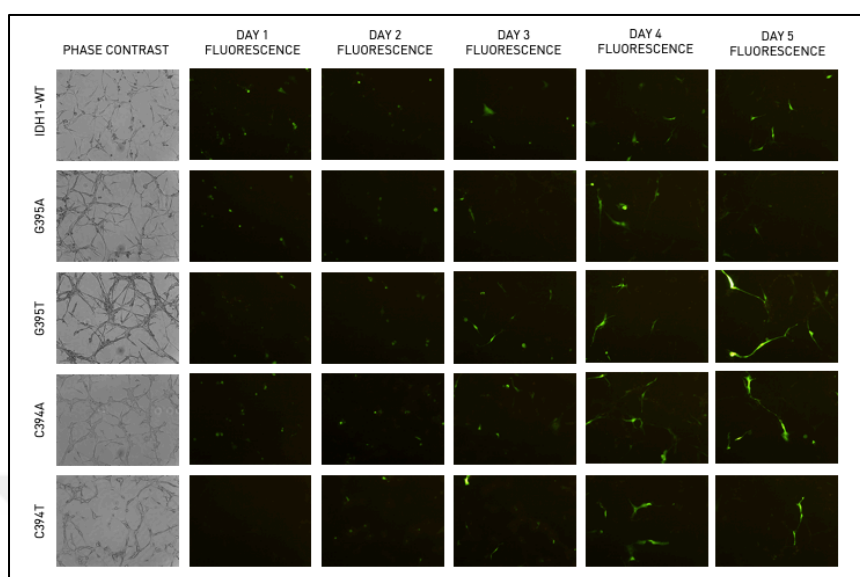**Figure 4.16: The fluorescence images of U87MG cells transfected
with PEI during MTT assay**

4.4 ANALYSIS OF IDH1 MUTATIONS EFFECTS ON CELL MIGRATION WITH SCRATCH REPAIR ASSAY

To understand the effects of IDH1 mutations on cell migration, scratch repair assay was performed to U87MG cells transfected with electroporation method and HCT cells transfected with PEI transfection process.

The cell images which were taken at 0, 8, and 24 hours after the scratch repair assay with U87MG cells are seen in Figure 4.17. It can be observed that the wound region formed in all experimental groups is close to closure. There is an increase in the closure of the area in each group, as seen in the migration index graphs generated by taking the percentages of the differences in the areas of each group, but there is no difference that can be associated with each other. Therefore, it can be interpreted that IDH1 mutations have no effect on cell migration in U87MG cells. Also, the graph showing the migration index is given in Figure 4.18.

Figure 4.17: The images of scratch repair assay with U87MG cells
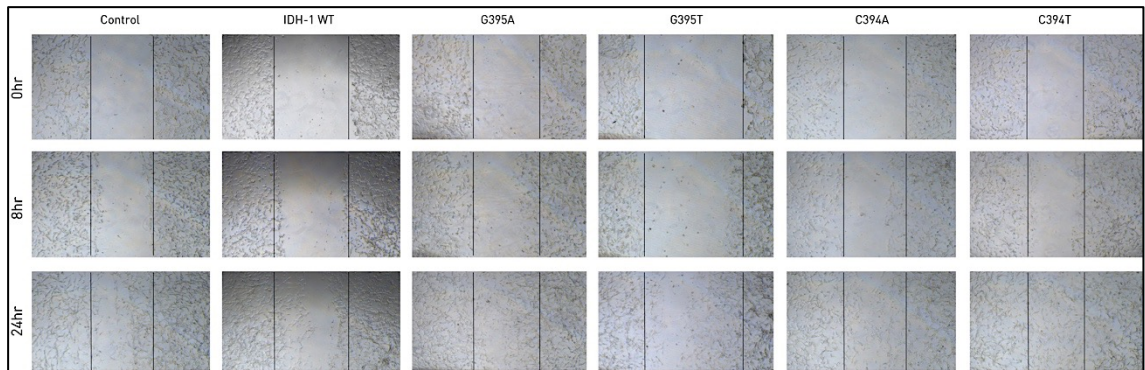
Reference: This photograph was taken by Gizem TURAN

Figure 4.18: The quantitative result of cell migration of U87MG cells
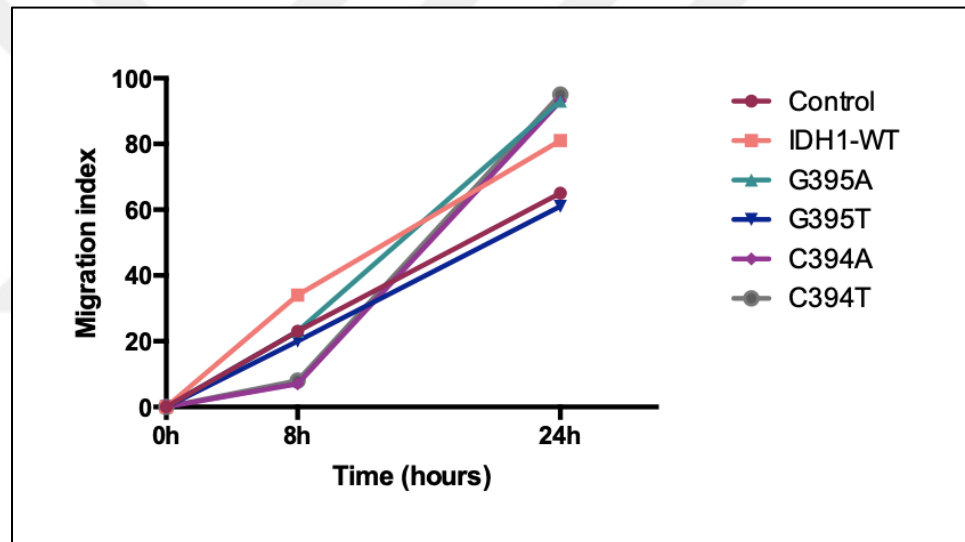
Reference: This photograph was taken by Gizem TURAN

Similar results were obtained in the scratch repair assay with HCT cells, as in U87MG cells. As shown in Figure 4.19, the scratched areas formed in the cells are close to closure and there is no relationship between the wildtype and mutation groups as seen in Figure 4.20. As a result, IDH1 mutations have no effect on cell migration in HCT cells.

Figure 4.19: The images of scratch repair assay with HCT cells
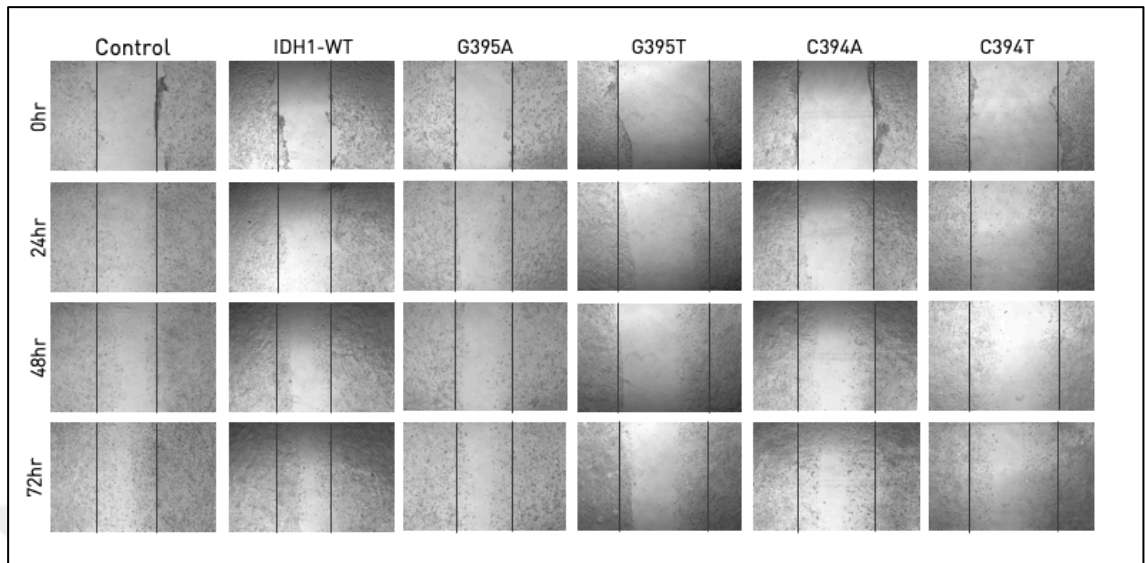

Reference: This photograph was taken by Gizem TURAN

Figure 4.20: The quantitative result of cell migration of HCT cells
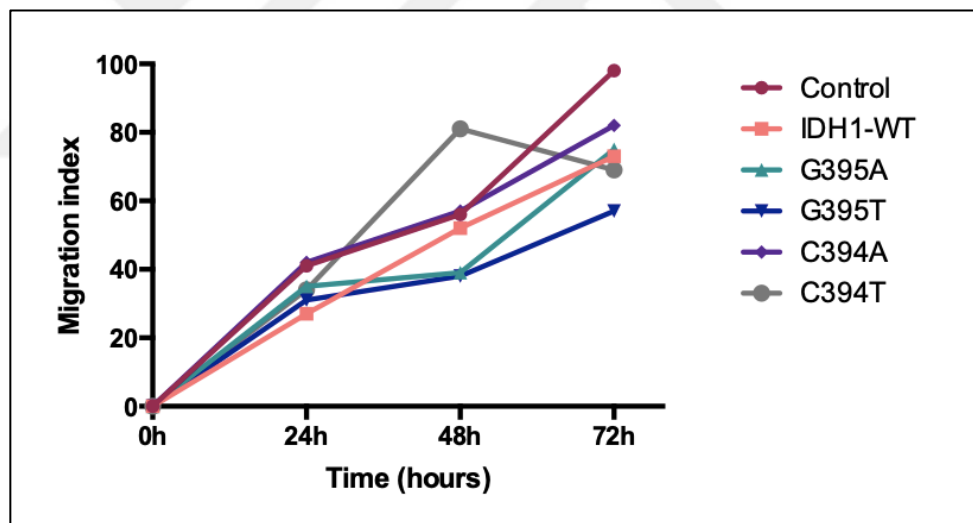
Reference: This photograph was taken by Gizem TURAN

4.5 DETECTION OF IDH1 WILDTYPE AND IDH1 MUTANT PROTEINS

Since GFP fluorescence was obtained in 293T cells and not obtained in U87MG cells, Western Blot assay was performed to confirm whether the IDH1 proteins were expressed in these cells. After Western Blot assay, HA-tag IDH1 proteins were detected from protein extracts from the cells transfected with IDH1 wildtype and IDH1 mutant

plasmids. Since the control group of U87MG cells was not transfected, this group did not contain our plasmids, and so HA-tag IDH1 proteins were not detected in this group. This confirms that the only our specific target proteins were identified. The result of Western Blot assay is seen in Figure 4.21.

Figure 4.21: The detection of HA-tag IDH1$^{\text{WT}}$ and IDH1$^{\text{MUT}}$ proteins
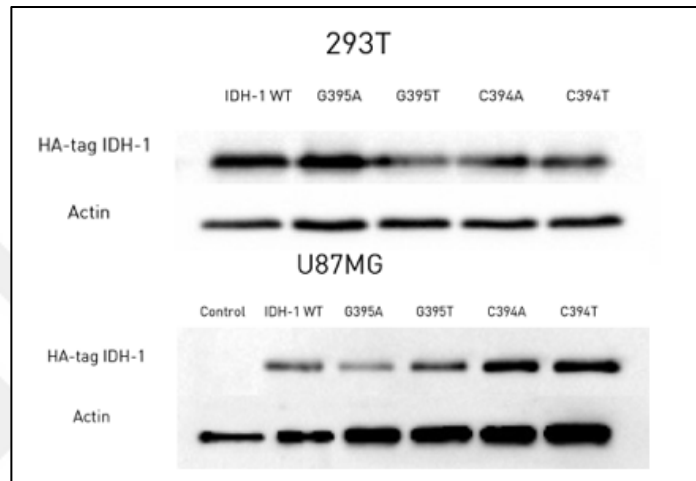
Reference: This photograph was taken by Gizem TURAN

5. CONCLUSION

In this study on IDH1 mutations that are very significant for the prognosis of glial tumors, the effects of these mutations on cell proliferation and migration were investigated and studies were performed to find the genotype-phenotype correlations. In our studies on cell proliferation, the effect of these IDH1 mutations in glioma cells on proliferation was not seen, the effect of C394T IDH1 mutation on reducing proliferation was observed as a result in non-glial cells. In both glioma and non-glial cell lines, it was concluded that IDH1 mutations had no effect on cell migration. To reinforce this study, in the future the same studies can be repeated with different primary glial tumor cells. In addition, in order to further examine whether the C394T mutation behaves differently from the other mutations, epigenetic regulations may be analyzed based on the TET family of DNA hydroxylases and the JmjC domain-containing histone demethylases.

REFERENCES

Periodicals

Al-Khallaf, H. 2017. Isocitrate dehydrogenases in physiology and cancer: biochemical and molecular insight. *Cell & bioscience,* **7,** 37.

Aquilanti, E., Miller, J., Santagata, S., Cahill, D. P. & Brastianos, P. K. 2018. Updates in prognostic markers for gliomas. *Neuro-oncology,* **20,** vii17-vii26.

Avşar, T. & Kiliç, T. Yüksek Gradeli Gliomların Moleküler Biyolojisi.

Behin, A., Hoang-Xuan, K., Carpentier, A. F. & Delattre, J.-Y. 2003. Primary brain tumours in adults. *The Lancet,* **361,** 323-331.

Bleeker, F. E., Atai, N. A., Lamba, S., Jonker, A., Rijkeboer, D., Bosch, K. S., Tigchelaar, W., Troost, D., Vandertop, W. P. & Bardelli, A. 2010. The prognostic IDH1 R132 mutation is associated with reduced NADP+-dependent IDH activity in glioblastoma. *Acta neuropathologica,* **119,** 487-494.

Buckner, J. C., Brown, P. D., O'neill, B. P., Meyer, F. B., Wetmore, C. J. & Uhm, J. H. Central nervous system tumors. Mayo Clinic Proceedings, 2007. Elsevier, 1271-1286.

Choi, C., Raisanen, J. M., Ganji, S. K., Zhang, S., Mcneil, S. S., An, Z., Madan, A., Hatanpaa, K. J., Vemireddy, V. & Sheppard, C. A. 2016. Prospective longitudinal analysis of 2-hydroxyglutarate magnetic resonance spectroscopy identifies broad clinical utility for the management of patients with IDH-mutant glioma. *Journal of Clinical Oncology,* **34,** 4030.

Chowdhury, R., Yeoh, K. K., Tian, Y. M., Hillringhaus, L., Bagg, E. A., Rose, N. R., Leung, I. K., Li, X. S., Woon, E. C. & Yang, M. 2011. The oncometabolite 2-hydroxyglutarate inhibits histone lysine demethylases. *EMBO reports,* **12,** 463-469.

Dang, L., White, D. W., Gross, S., Bennett, B. D., Bittinger, M. A., Driggers, E. M., Fantin, V. R., Jang, H. G., Jin, S. & Keenan, M. C. 2009. Cancer-associated IDH1 mutations produce 2-hydroxyglutarate. *Nature,* **462,** 739.

Deangelis, L. M. 2001. Brain tumors. *New England Journal of Medicine,* **344,** 114-123.

Deberardinis, R. J., Lum, J. J., Hatzivassiliou, G. & Thompson, C. B. 2008. The biology of cancer: metabolic reprogramming fuels cell growth and proliferation. *Cell metabolism,* **7,** 11-20.

Deng, L., Xiong, P., Luo, Y., Bu, X., Qian, S., Zhong, W. & Lv, S. 2018. Association between IDH1/2 mutations and brain glioma grade. *Oncology letters,* **16,** 5405-5409.

Eckel-Passow, J. E., Lachance, D. H., Molinaro, A. M., Walsh, K. M., Decker, P. A., Sicotte, H., Pekmezci, M., Rice, T., Kosel, M. L. & Smirnov, I. V. 2015. Glioma groups based on 1p/19q, IDH, and TERT promoter mutations in tumors. *New England Journal of Medicine,* **372,** 2499-2508.

Esteller, M., Garcia-Foncillas, J., Andion, E., Goodman, S. N., Hidalgo, O. F., Vanaclocha, V., Baylin, S. B. & Herman, J. G. 2000. Inactivation of the DNA-repair gene MGMT and the clinical response of gliomas to alkylating agents. *New England Journal of Medicine,* **343,** 1350-1354.

Filipp, F. V., Scott, D. A., Ronai, Z. E. A., Osterman, A. L. & Smith, J. W. 2012. Reverse TCA cycle flux through isocitrate dehydrogenases 1 and 2 is required for lipogenesis in hypoxic melanoma cells. *Pigment cell & melanoma research,* **25,** 375-383.

Hartmann, C., Meyer, J., Balss, J., Capper, D., Mueller, W., Christians, A., Felsberg, J., Wolter, M., Mawrin, C. & Wick, W. 2009. Type and frequency of IDH1 and IDH2 mutations are related to astrocytic and oligodendroglial differentiation and age: a study of 1,010 diffuse gliomas. *Acta neuropathologica,* **118,** 469-474.

Hausinger, R. P. 2004. Fe (II)/α-ketoglutarate-dependent hydroxylases and related enzymes. *Critical reviews in biochemistry and molecular biology,* **39,** 21-68.

Hegi, M. E., Diserens, A.-C., Godard, S., Dietrich, P.-Y., Regli, L., Ostermann, S., Otten, P., Van Melle, G., De Tribolet, N. & Stupp, R. 2004. Clinical trial substantiates the predictive value of O-6-methylguanine-DNA methyltransferase promoter methylation in glioblastoma patients treated with temozolomide. *Clinical cancer research,* **10,** 1871-1874.

Huang, F. W., Hodis, E., Xu, M. J., Kryukov, G. V., Chin, L. & Garraway, L. A. 2013. Highly recurrent TERT promoter mutations in human melanoma. *Science,* **339,** 957-959.

Khurshed, M., Molenaar, R. J., Lenting, K., Leenders, W. P. & Van Noorden, C. J. 2017. In silico gene expression analysis reveals glycolysis and acetate anaplerosis in IDH1 wild-type glioma and lactate and glutamate anaplerosis in IDH1-mutated glioma. *Oncotarget,* **8,** 49165.

Kim, J. H., Lee, S.-R., Li, L.-H., Park, H.-J., Park, J.-H., Lee, K. Y., Kim, M.-K., Shin, B. A. & Choi, S.-Y. 2011. High cleavage efficiency of a 2A peptide derived from porcine teschovirus-1 in human cell lines, zebrafish and mice. *PLoS one,* **6,** e18556.

Kim, S. Y., Lee, S. M., Tak, J. K., Choi, K. S., Kwon, T. K. & Park, J.-W. 2007. Regulation of singlet oxygen-induced apoptosis by cytosolic NADP+-dependent isocitrate dehydrogenase. *Molecular and cellular biochemistry,* **302,** 27-34.

Kranendijk, M., Struys, E. A., Salomons, G. S., Van Der Knaap, M. S. & Jakobs, C. 2012. Progress in understanding 2-hydroxyglutaric acidurias. *Journal of inherited metabolic disease,* **35,** 571-587.

Lapointe, S., Perry, A. & Butowski, N. A. 2018. Primary brain tumours in adults. *The Lancet.*

Lee, J. H., Kim, S. Y., Kil, I. S. & Park, J.-W. 2007. Regulation of ionizing radiation-induced apoptosis by mitochondrial NADP+-dependent isocitrate dehydrogenase. *Journal of biological chemistry,* **282,** 13385-13394.

Lemons, J. M., Feng, X.-J., Bennett, B. D., Legesse-Miller, A., Johnson, E. L., Raitman, I., Pollina, E. A., Rabitz, H. A., Rabinowitz, J. D. & Coller, H. A. 2010. Quiescent fibroblasts exhibit high metabolic activity. *PLoS biology,* **8,** e1000514.

Loenarz, C. & Schofield, C. J. 2008. Expanding chemical biology of 2-oxoglutarate oxygenases. *Nature chemical biology,* **4,** 152.

Losman, J.-A. & Kaelin, W. G. 2013. What a difference a hydroxyl makes: mutant IDH,(R)-2-hydroxyglutarate, and cancer. *Genes & development,* **27,** 836-852.

Louis, D. N., Ohgaki, H., Wiestler, O. D., Cavenee, W. K., Burger, P. C., Jouvet, A., Scheithauer, B. W. & Kleihues, P. 2007. The 2007 WHO classification of tumours of the central nervous system. *Acta neuropathologica,* **114,** 97-109.

Louis, D. N., Perry, A., Reifenberger, G., Von Deimling, A., Figarella-Branger, D., Cavenee, W. K., Ohgaki, H., Wiestler, O. D., Kleihues, P. & Ellison, D. W. 2016. The 2016 World Health Organization classification of tumors of the central nervous system: a summary. *Acta neuropathologica,* **131,** 803-820.

Lu, C., Ward, P. S., Kapoor, G. S., Rohle, D., Turcan, S., Abdel-Wahab, O., Edwards, C. R., Khanin, R., Figueroa, M. E. & Melnick, A. 2012. IDH mutation impairs histone demethylation and results in a block to cell differentiation. *Nature,* **483,** 474.

Molenaar, R. J., Radivoyevitch, T., Maciejewski, J. P., Van Noorden, C. J. & Bleeker, F. E. 2014. The driver and passenger effects of isocitrate dehydrogenase 1 and 2 mutations in oncogenesis and survival prolongation. *Biochimica et Biophysica Acta (BBA)-Reviews on Cancer,* **1846,** 326-341.

Noushmehr, H., Weisenberger, D. J., Diefes, K., Phillips, H. S., Pujara, K., Berman, B. P., Pan, F., Pelloski, C. E., Sulman, E. P. & Bhat, K. P. 2010. Identification of a CpG island methylator phenotype that defines a distinct subgroup of glioma. *Cancer cell,* **17,** 510-522.

Ohgaki, H. & Kleihues, P. 2013. The definition of primary and secondary glioblastoma. *Clinical cancer research,* **19,** 764-772.

Ostrom, Q. T., Gittleman, H., Liao, P., Vecchione-Koval, T., Wolinsky, Y., Kruchko, C. & Barnholtz-Sloan, J. S. 2017. CBTRUS statistical report: primary brain and other central nervous system tumors diagnosed in the United States in 2010–2014. *Neuro-oncology,* **19,** v1-v88.

Reitman, Z. J. & Yan, H. 2010. Isocitrate dehydrogenase 1 and 2 mutations in cancer: alterations at a crossroads of cellular metabolism. *Journal of the National Cancer Institute,* **102,** 932-941.

Struys, E. A., Salomons, G. S., Achouri, Y., Van Schaftingen, E., Grosso, S., Craigen, W. J., Verhoeven, N. M. & Jakobs, C. 2005. Mutations in the D-2-hydroxyglutarate dehydrogenase gene cause D-2-hydroxyglutaric aciduria. *The American Journal of Human Genetics,* **76,** 358-360.

Togao, O., Hiwatashi, A., Yamashita, K., Kikuchi, K., Mizoguchi, M., Yoshimoto, K., Suzuki, S. O., Iwaki, T., Obara, M. & Van Cauteren, M. 2015. Differentiation of high-grade and low-grade diffuse gliomas by intravoxel incoherent motion MR imaging. *Neuro-oncology,* **18,** 132-141.

Turcan, S., Rohle, D., Goenka, A., Walsh, L. A., Fang, F., Yilmaz, E., Campos, C., Fabius, A. W., Lu, C. & Ward, P. S. 2012. IDH1 mutation is sufficient to establish the glioma hypermethylator phenotype. *Nature,* **483,** 479.

Wen, P. Y. & Kesari, S. 2008. Malignant gliomas in adults. *New England Journal of Medicine,* **359,** 492-507.

Wesseling, P. & Capper, D. 2018. WHO 2016 classification of gliomas. *Neuropathology and applied neurobiology,* **44,** 139-150.

Xu, W., Yang, H., Liu, Y., Yang, Y., Wang, P., Kim, S.-H., Ito, S., Yang, C., Wang, P. & Xiao, M.-T. 2011. Oncometabolite 2-hydroxyglutarate is a competitive inhibitor of α-ketoglutarate-dependent dioxygenases. *Cancer cell,* **19,** 17-30.

Xu, X., Zhao, J., Xu, Z., Peng, B., Huang, Q., Arnold, E. & Ding, J. 2004. Structures of human cytosolic NADP-dependent isocitrate dehydrogenase reveal a novel self-regulatory mechanism of activity. *Journal of Biological Chemistry,* **279,** 33946-33957.

Yan, H., Parsons, D. W., Jin, G., Mclendon, R., Rasheed, B. A., Yuan, W., Kos, I., Batinic-Haberle, I., Jones, S. & Riggins, G. J. 2009. IDH1 and IDH2 mutations in gliomas. *New England Journal of Medicine,* **360,** 765-773.

Yeole, B. B. 2008. Trends in the brain cancer incidence in India. *Asian Pac J Cancer Prev,* **9,** 267-270.

Ying, W. 2008. NAD+/NADH and NADP+/NADPH in cellular functions and cell death: regulation and biological consequences. *Antioxidants & redox signaling,* **10,** 179-206.

Zhao, S., Lin, Y., Xu, W., Jiang, W., Zha, Z., Wang, P., Yu, W., Li, Z., Gong, L. & Peng, Y. 2009. Glioma-derived mutations in IDH1 dominantly inhibit IDH1 catalytic activity and induce HIF-1α. *Science,* **324,** 261-265.